Summer 2016

Carbon Deposition During Oxygen Production Using High Temperature Electrolysis and Mitigation Methods

Timothy Adam Bernadowski
Old Dominion University

CARBON DEPOSITION DURING OXYGEN PRODUCTION USING HIGH TEMPERATURE ELECTROLYSIS AND MITIGATION METHODS

by

Timothy Adam Bernadowski, Jr.
B.S. May 2015, Old Dominion University

A Thesis Submitted to the Faculty of
Old Dominion University in Partial Fulfillment of the
Requirements for the Degree of

MASTER OF SCIENCE IN MECHANICAL ENGINEERING

OLD DOMINION UNIVERSITY
August 2016

Approved By:

Xiaoyu Zhang (Director)

Robert L. Ash (Member)

Drew Landman (Member)

Abstract

CARBON DEPOSITION DURING OXYGEN PRODUCTION USING HIGH TEMPERATURE ELECTROLYSIS AND MITIGATION METHODS

Timothy Adam Bernadowski, Jr.
Old Dominion University, 2016
Director: Dr. Xiaoyu Zhang

Carbon dioxide in the Martian atmosphere can be converted to oxygen during high temperature electrolysis for use in life-support and fuel systems on manned missions to the red planet. During electrolysis of carbon dioxide to produce oxygen, carbon can deposit on the electrolysis cell resulting in lower efficiency and possibly cell damage. This would be detrimental, especially when the oxygen product is used as the key element of a space life support system. In this thesis, a theoretical model was developed to predict hazardous carbon deposition conditions under various operating conditions within the Martian atmosphere. The model can be used as a guide to determine the ideal operating conditions of the high-temperature oxygen production system. A parallel experimental investigation is underway to evaluate the accuracy of the theoretical model. The experimental design, cell fabrication, and some preliminary results as well as future work recommendations are also presented in this thesis.

Acknowledgments

I would like to thank the Virginia Space Grant Consortium for their support of my project and my schooling throughout this past year. I would like to extend a special thank you to my Director and Graduate Advisor, Dr. Xiaoyu Zhang who was able to give me this unique research opportunity and present me with much encouragement, support, and many opportunities to enrich my learning along the way, from undergraduate to graduate levels. I would also like to thank my Undergraduate Advisor, Dr. Drew Landman, who always supported me throughout my entire university experience. To the third member of my committee, Dr. Robert Ash, I am particularly grateful for truly challenging me to rise up to the high demands of graduate school as I prepared to transition from undergraduate senior to graduate student. Throughout the experimental portions of this study I had the pleasure of working with lab partners Can Zhou and Todd Spreeman. Without them, I would not have gotten as far as I did. I would also like to acknowledge the support I had from the faculty of the Mechanical & Aerospace Engineering Department here at ODU, from the teaching assistantship that made it possible for me to continue my schooling to all the education along the way. I would like to mention my good friend Angelo Espiritu who came through in my time of need to help me understand some of the chemistry involved in this thesis. Lastly, but certainly not least, I would like to thank my parents, sister, and loving fiancée, Samantha, for their ever present inspiration and support throughout everything, academically and beyond.

Nomenclature

HTE	High Temperature Electrolysis
NASA	National Aeronautics and Space Administration
CO_2	Carbon Dioxide
CO	Carbon Monoxide
O_2	Oxygen
C	Carbon
SOEC	Solid Oxide Electrolysis Cell
SOFC	Solid Oxide Fuel Cell
R&D	Research & Development
LTE	Low Temperature Electrolysis
H_2O	Water (Steam)
H_2	Hydrogen
NO_x	Nitrous Oxide
V_N	Nernst Potential
V^0	Nernst Potential at standard conditions
R_U	Ideal gas constant
T	Cell temperature
j	Number of moles electrons transferred
F	Faraday's constant
y_{CO_2}	Partial pressure of CO_2
y_{CO}	Partial pressure of CO

y_{O_2}	Partial pressure of O_2
P	Experimental pressure
P_{std}	Standard pressure
Δg	Gibbs Energy
Δh	Enthalpy
Δs	Entropy
YSZ	Yttria-stabilized Zirconia (electrolyte material)
V	Volts
ISRU	*In-Situ* Resource Utilization (system)
LSM	$La_{1-x}Sr_xMnO_3$ (oxygen electrode material)
LSCM	$La_{1-x}Sr_xCr_{0.5}Mn_{0.5}O_3$ (oxygen electrode material)
LSV	$La_{1-x}Sr_xV_{0.9}O_3$ (oxygen electrode material)
LSCF	$La_{0.6}Sr_{0.4}Co_{0.2}Fe_{0.8}O_{3-\delta}$ (oxygen electrode material)
BSCF	$Ba_{0.5}Sr_{0.5}Co_{0.8}Fe_{0.2}O_{3-\delta}$ (oxygen electrode material)
LCC	$LaCrO_3$ (oxygen electrode material)
HTSE	High Temperature Steam Electrolysis
INL	Idaho National Laboratory
EIFER	European Institute for Energy Research
CEA	Alternative Energies and Atomic Energy Commission
INET	Institute of Nuclear and New Energy Technology
DOE	United States' Department of Energy
NGNP	Next Generation Nuclear Plant
HTGR	High Temperature Gas-cooled Reactor

NIMTE	Ningbo Institute of Materials Technology and Engineering
RTG	Radioisotope Thermoelectric Generator

Table of Contents

List of Tables

List of Figures

Chapter 1

Introduction

Supplying oxygen for humans while on missions to Mars is a key factor in making human exploration of Mars possible. While Earth's atmosphere consists of 21% oxygen, Mars has only trace amounts of oxygen. In comparison, carbon dioxide is abundant in the Martian atmosphere, accounting for over 95% [1-4]. Transporting oxygen to Mars is expensive and impractical as the volume of oxygen tanks required would be too large to be a viable option considering the space, weight, and structural limitations of spacecraft. An estimate of 75% of the payload weight would be oxygen in that case [3]. Alternatively, it is more practical to produce the required oxygen (i.e. 1 kilogram of oxygen needed per astronaut per day [5]) on Mars using Martian resources (*in-situ*), which in turn reduces the required payload of a manned mission to Mars by 75% [6].

Producing oxygen on Mars using high temperature electrochemical separation is not a novel idea. The concept has been investigated for more than two decades and was initially proposed by Stancati *et al.* in 1979 [7]. The next Mars rover, set to launch in 2020, will carry an apparatus called MOXIE (Mars Oxygen In-Situ Resources Utilization Experiment) that will be built by the Massachusetts Institute of Technology (MIT) and NASA's Jet Propulsion Laboratory (JPL). MOXIE will demonstrate that oxygen can indeed be produced via high temperature electrolysis (HTE) using solid oxide electrolysis cells (SOECs) on Mars for the first time [3, 4]. The oxygen produced by MOXIE would have several potential uses including life support and return trip oxidant [4]. Pending successful demonstration of MOXIE on the 2020 launch, a larger unit would be sent to Mars on the next mission, and would start generating and storing

oxygen for future missions to Mars [3, 4, 8]. MOXIE is expected to produce about 22 grams of oxygen per hour through high temperature CO_2 electrolysis using SOECs [8]. MOXIE compensates for the low pressure of Mars by cryogenically compressing the Martian CO_2 and then introducing compressed CO_2 into the system [8].

Although high temperature CO_2 electrolysis is able to produce oxygen, a potential problem is that the chemical reaction can proceed along two pathways. Carbon dioxide can be split into either oxygen and carbon monoxide (pathway (1)) or solid carbon and oxygen (pathway (2)). In addition, pathway (3) is also viable, as CO is a byproduct of pathway (1).

$$CO_2(g) \rightarrow CO(g) + \frac{1}{2}O_2(g) \quad (1)$$

$$CO_2(g) \rightarrow C(s) + O_2(g) \quad (2)$$

$$CO(g) \rightarrow C(s) + \frac{1}{2}O_2(g) \quad (3)$$

Pathway (2) and (3) are unfavorable, since solid carbon will adsorb onto the electrodes in both reactions. Carbon deposition reduces the catalyst active area and the electrode porosity, resulting in performance degradation [9-11]. Generally, the relationship between carbon deposition and performance degradation is remarkably higher when the process is operated at high current density or high temperature [10, 11]. Carbon deposition should therefore be characterized at the conditions that would simulate operation on Mars.

The key component of the HTE process is the SOEC. Theoretically an electrolysis cell is a fuel cell operated in the reverse mode [9, 12, 13]. A typical SOEC consists of two electrodes sandwiching an oxygen ion conductive electrolyte (shown in Figure 1.1). In an ideal HTE

process (pathway 1), CO_2 combines electrons and dissociates into O^{2-} ions and CO on the cathode. O^{2-} ions migrate through the electrolyte to the anode, where they evolve as oxygen gas and release electrons. CO is a byproduct and is usually vented out [9, 12-16]. Due to the solid state electrolyte (gas impermeable), SOECs are able to produce very pure oxygen without using filters or absorbers in many cases [17].

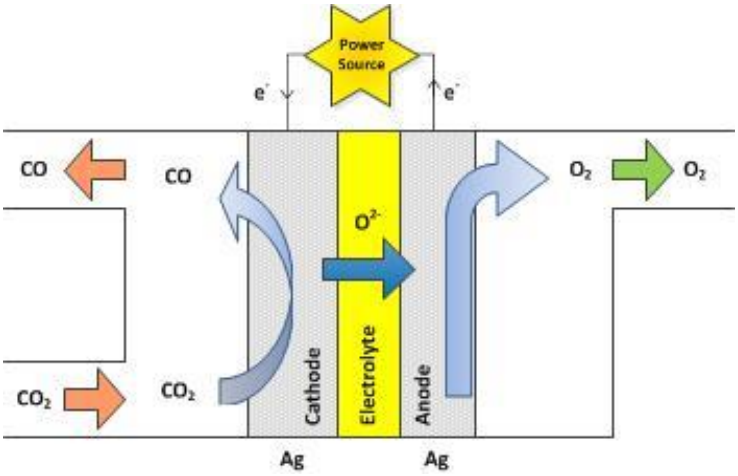

Figure 1.1: Schematic diagram of SOEC used in this thesis for carbon dioxide electrolysis.

1.1 Thesis Statement

The main objective of this thesis was to establish a thermodynamic model to identify the Martian operating conditions that would result in hazardous carbon deposition during high temperature CO_2 electrolysis. The model simulated the Martian conditions (mainly the partial pressure of CO_2, characterizing Mars atmosphere) and predicted the electrolysis pathways subject to these conditions. This model was employed to determine favorable operating

conditions for SOECs that cause pathway (1) to be dominant. The model was then utilized to guide the experimental investigation.

1.2 Organization

This thesis consists of five chapters, including the Introduction. The second chapter contains a comprehensive literature review, defining and discussing the different variables and parameters that control SOEC operation. The theoretical analysis is developed in Chapter 3, using fuel cell theory to evolve the thermodynamic model for identifying the conditions under which solid carbon deposition occurs. Chapter 4 discusses preliminary experimental results from this study. Chapter 5 contains the conclusions and discusses recommendations for future work.

Chapter 2

Literature Review

2.1 Generating Oxygen via High Temperature Electrolysis

The history of HTE is related to the research and development (R&D) of the solid oxide fuel cell (SOFC). Following the oil crisis in 1970s, Doenitz *et al.* looked into a large-scale hydrogen production funded by so called 'Hot Elly' project using high temperature steam electrolysis [18]. Due to technical limitations, initially tubular configurations were chosen for scaling up the design [19]. Subsequently, modular HTE units were developed and demonstrated, but without any long-term operation [20]. At the end of that project, the concepts for a prototype plant with 3.5 kW hydrogen output power were proposed [21]. After that, research on high temperature steam electrolysis remained quiet for nearly two decades. In the meantime, worldwide R&D on SOFCs had gone through an impressive progress. Recently, energy supply and global warming concerns have renewed the research on high temperature steam electrolysis using advanced technologies of solid-oxide cells [22-25].

While the global research focus of HTE has been clean fuel (hydrogen and syngas) production, NASA however has been more interested in oxygen production of such process. Manned spacecraft, flown by NASA, have been using electrolysis and fuel cells, starting with the Gemini dual-pilot orbit missions and continuing through the Apollo lunar missions and the International Space Station, where they are employed currently in water electrolysis mode to generate breathable oxygen for the astronauts on board [26-29]. The hydrogen produced in this process is saved for reaction with CO_2, exhaled by the astronauts, to produce water via Sabatier reaction[29, 30]. Given the long history of successful electrolysis cell implementation in space,

it is not surprising that a similar electrochemical approach is being considered for use in missions to Mars.

Stancati *et al.* [7] first proposed utilizing HTE for oxygen production at Mars employing only its atmosphere as feedstock. That study recognized that by transporting methane from Earth, oxygen could be produced *in* situ on Mars, which could constitute nearly 80 percent of the return vehicle propellant mass, resulting in dramatic reductions in initial Earth-launched payload requirement [7]. Two "In Situ Propellant Production" systems were proposed [7]. The first system produced oxygen through reduction of carbon dioxide, in which carbon monoxide was produced as a byproduct. A combined fuel of carbon dioxide and water to create oxygen and methane was proposed in the second system, which was also discussed in [5, 31, 32]. A system of this type would be advantageous since oxygen and methane would be useful as oxidizer and fuel to propel the return trip rocket [31]. Those systems were evaluated and found to be more economical and practical than an Orbit Capture system, which temporarily abandons fuel for the return trip from Mars to Earth in orbit and rendezvouses when ready to return, primarily because of the ability to lower payload weight when taking off from Mars and Earth [7]. The two systems proposed in [7] were also advantageous because of their ability to utilize the additional space previously reserved for return trip fuel for other electrical, chemical, and power systems which would be necessary on Mars.

Electrochemical conversion of CO_2 to O_2 for Martian applications using solid oxide cells, as suggested in [7] was pursued further at Jet Propulsion Laboratory by Robert Richter who modeled SOEC behavior during CO_2 reduction and experimentally verified his model [33]. Richter's study utilized thermally dissociating carbon dioxide in contact with an 8% yittria stabilized zirconia (8YSZ) cell, sandwiched between porous platinum electrodes. Although

those tests successfully extracted oxygen from the carbon dioxide feedstock, the applied voltages were higher than had been predicted by the model [33]. This increased voltage was considered to be the result of resistances and overpotentials [33]. The cell resistances mainly came from the thick electrolyte used back then, since the electrolyte needed to be thick enough to provide significant mechanical support. As a comparison, most commercial SOFCs nowadays use electrode supported cells that consists of a very thin layer of electrolyte. The Pt electrodes however contributed much less to the overall resistance as they are metallic. Furthermore, the significance of the overpotential was related to gas diffusion resistance (electrochemical resistance). High overpotentials could have happened when fuel starvation occurred on the electrodes for oxygen extraction due to limited porosity, low gas partial pressures, or/and low flow rates.

Undergraduate students at Old Dominion University have been involved in solid oxide oxygen processor system research and design since 1986 [34]. Using funds provided by the Planetary Society, a capstone design team designed and built a yttria stabilized zirconia system to investigate the feasibility of extracting oxygen directly from simulated Mars atmosphere [34]. The tubular electrolysis cell was procured from Ceramatec, and the Mars simulant feedstock matched the carbon dioxide and nitrogen content but substituted extra argon for the remaining components of Mars atmosphere [34]. That cell was operated at 1,000 K and in 1988, they were able to produce an oxygen yield with a reliable conversion efficiency of less than 25% [34]. Though operation was less than optimal, the study served as a proof of concept that a Mars oxygen processor was possible [34].

Frisbee *et al.* [35]proposed using the reverse water gas shift process to generate oxygen from Martian CO_2, by incorporating terrestrial hydrogen. The reverse water gas shift process

involves reduction of CO_2 and hydrogen to carbon monoxide (which could be used as rocket fuel) and water. Then standard water electrolysis is used to produce oxygen and hydrogen [5, 32, 35, 36]. The use of hydrogen as product and reactant poses an advantageous recycling system that could be utilized. However, a downside is that it requires an external hydrogen supply [32]. Furthermore, the reverse water gas shift process needs high temperature (400°C to 650°C [5]) during operation and therefore demands a considerable amount of thermal energy input. In addition, water electrolysis process also consumes significant amount of electrical energy. As an example, the system in Reference [35] would need 33.8 kW of power. Due to the low system reliability, Frisbee *et al.* proposed three different modifications, including eliminating rotating machinery, adding backup components in case of failure, and improving zirconia cell efficiency as it consumed the majority of the input power [35].

During the 1990's, several studies were conducted by Sridhar *et al.* in preparation for their planned 2001 Mars Surveyor Mission [37-40]. In those studies, SOECs were utilized to support a Sabatier reactor and water electrolysis system to utilize CO_2 harvested from the atmosphere of Mars and hydrogen transported from Earth to generate water and oxygen [37-39, 41]. This system utilized a two-step process. The first step used a Sabatier reaction to produce methane and water [37]. The second step was water electrolysis to produce hydrogen and oxygen, the former of which can be recycled and used in the first step again [37]. One potential problem with this system is the need to have a ready supply of hydrogen brought from Earth, which would need to be accounted for in the payload weight and would take up space in the spacecraft, although the hydrogen produced as a result of water electrolysis could potentially be processed and reused in the Sabatier reactor [5, 38]. With the failure of the Mars Polar Lander and Climate Orbiter missions, the Mars Surveyor Lander mission was cancelled and the

equipment was never tested on Mars, leading to a general wane in public interested in solid oxide technology. Tao *et al.* continued these studies and investigated the effects of CO_2 electrolysis on the electrode/electrolyte interface [42, 43]. These studies utilized electrolyte (8YSZ) supported cells with porous platinum/YSZ cermet electrodes [43]. The performance of Pt-YSZ based SOECs were characterized using V-I sweeps under different temperatures ranging from 1023 to 1123 K [43]. However, no results of long-term testing were reported to demonstrate the durability of the SOECs and potential carbon deposition at the single cell level.

While high temperature fuel cell/electrolysis technology advanced significantly, several sources focused on updates to *in-situ* resource utilization systems on Mars [44-46]. The concept of producing oxygen *in-situ* on Mars was discussed in depth by Rapp [5]. For a 6-person crew stay to stay for 600 days on Mars, 6.8 metric tons of oxygen would be required if no *In-Situ* Resource Utilization system (ISRU) or recycling process was employed [5]. To compensate for this heavy demand, Rapp suggested utilizing an ISRU system that would be sent months ahead of the manned mission low Earth orbit departure date. This ISRU would begin the oxygen generation process and have a stockpile of oxygen by the time the manned mission lands on Mars. This is the same concept discussed in [3, 4, 8] with regards to MOXIE. One potential process for generating oxygen that was discussed in [37] was also discussed in [5]: they use of a combined Sabatier / water electrolysis process which could have an approximate 95% methane and oxygen yield [5]. Additionally SOEC conversion of CO_2 to O_2 using chemical reaction (1) was discussed. For the given mission length and crew demand, Rapp calculated that 1540 Yttria-stabilized zirconia (YSZ) wafers (single SOECs) would be necessary in order to support the manned mission [5]. Rapp also discussed the power requirement for various oxygen production rates and the possibility for a highly efficient CO_2 conversion rate (very close to 100%) [5]. An

O_2 production rate of 1 kg/hr would require a current of 12,300 Amperes, thus creating a power requirement range of 12,300 Watts (with per cell electrolysis voltage at 1.0 Volts) – 18450 Watts (with per cell electrolysis voltage at 1.5 Volts) [5]. Many of the systems mentioned in Reference [5] utilize a CO_2 compression system before introducing the CO2 feedstock to the SOEC, making the operating conditions of the SOEC system on Mars similar to operation on Earth.

In order to increase SOEC reliability, which was a major issue in many early tests, new SOEC materials (mostly ceramics) and their effects on cell performance were studied. Many of these ceramics were used to strengthen the seals of the SOECs (which would fail in high temperature conditions). These new types of ceramic electrodes included, LSCM ($La_{0.8}Sr_{0.2}Cr_{0.5}Mn_{0.5}O_3$), LCC ($LaCrO_3$), LSCF ($La_{0.6}Sr_{0.4}Co_{0.2}Fe_{0.8}O_{3-\delta}$), BSCF ($Ba_{0.5}Sr_{0.5}Co_{0.8}Fe_{0.2}O_{3-\delta}$), and LSV ($La_{0.7}Sr_{0.3}V_{0.9}O_3$) have helped to improve cell reliability as they are stronger than their traditional counterparts [47-52]. This strength allows many of these new materials to withstand the large pressure differences the oxygen ions produce as they pass through the electrode/electrolyte interfaces during operation in electrolysis mode, leading to tests greater than 1,000 hours in length [53]. Another advantage of these ceramic electrodes of particular interest to this investigation, is LSCM's ability to combat carbon deposition [48]. Many of these studies were conducted at NASA Glenn with cell materials manufactured by Ceramatec Inc. and Materials and Systems Research Inc. with Paragon Space Development Corporation getting into the game as well with their combination SOEC/Sabatier reactor stacks [30, 53, 54]. All of these recent technological advances have made the MOXIE project, outlined in [3, 4, 8], more viable today than it would have been decades ago.

However, practically there are two disadvantages of the layout of previously proposed system as well as MOXIE that used compressed CO_2 as the feedstock. First, a Martian CO_2 capture and storage unit needs to be included, which adds up additional payload [55]. Second, the pressure difference between the SOEC chamber and Martian ambient environment is detrimental to the ceramic or glass based sealing [25]. Those two practical concerns result in the initial thought of simulating real Martian conditions for the theoretical and experimental research in this thesis. Since it was first suggested in [7], there have been many studies and discussions regarding oxygen generation using SOEC technology, Sabatier/electrolysis systems, and reverse water gas shift processes with the intent for use on manned missions to Mars. However, there is limited information regarding the optimized operating conditions of SOECs at Martian atmospheric conditions. Thus, in order to ensure successful implementation of SOEC technology on Mars, there is a direct need to develop models to simulate the performance of SOECs on Mars. As mentioned before, one concern is carbon deposition during the operation of SOEC technology on Mars. To address the potentially hazardous problem, analysis of the Martian operating conditions of SOECs is needed. Hereby, the operating variables, including cell temperature, fuel composition, geometric setup, and electrolysis voltage are discussed in the following sections.

2.2 High or Low Temperature Electrolysis

Electrolysis process consumes both electrical and thermal energy. In terms of thermodynamics, during electrolysis the electrical energy requirement (change of Gibbs free energy) decreases while the thermal energy requirement ($T\Delta S$) increases with increasing temperature [56]. Electrolysis can therefore be categorized into low and high temperature, based

on operating temperatures. Electrolysis cells usually are constrained in a certain range of operating temperatures due to their electrochemical configurations and material properties, which are elaborated in the following sections. Furthermore, the reason why high temperature electrolysis is the only viable technology for CO_2 electrolysis is discussed.

2.2.1 Low Temperature Electrolysis

Low temperature electrolysis (LTE) relies on proton exchange membrane (PEM) or alkaline cells to maintain the electrolysis of water to produce oxygen. Alkaline water electrolysis has been around since 1789 and uses a diaphragm to separate two electrodes submerged in a liquid alkaline electrolyte [57, 58]. While this was discovered first and is used in industry today, most of the current research is focused on the PEM cell. PEM technology has several advantages over alkaline cells including higher efficiency and higher current density (which leads to a more compact design than alkaline cells) as well as lower gas crossover due to the material structure of the membrane [57]. One disadvantage of PEM technology over alkaline technology is cost, as PEM cells currently require expensive materials, such as usually using platinum as a catalyst, to operate [57]. Due to the high interest in PEM technology leading to greater manufacturing demand, these prices are expected to decrease over time, increasing the viability of PEM cells over alkaline cells [57]. LTE has been utilized in space for oxygen generation already, providing the advantage of familiarity when considering it for use on Mars [26].

Since the membranes that support LTE technology cannot conduct oxygen ions, a CO_2 feedstock cannot be used which would mean that the feedstock (water in this case) would have to be brought from Earth [22]. Additionally, LTE technology cannot take advantage of the higher

efficiencies and lower power demand offered by HTE options because the electrolysis of water is more endothermic with increasing temperatures [57].

2.2.2 High Temperature Electrolysis

High temperature electrolysis uses SOECs that usually operate at temperatures above 750°C with higher thermodynamic efficiency as compared to LTE cells [9, 22, 42, 59-61]. High temperatures are needed because the electrolyte materials used in SOECs only become obviously ionic conductive at elevated temperatures (usually above 700 C°) [62]. Furthermore, the anode (usually made of metal oxides) also needs high temperatures to reach good electric conductivity. Another advantage of operating at high temperatures is that the activation energy (overpotentials) on the electrodes become much less than those at low temperatures (i.e. water electrolysis), resulting in much less electrical energy input. For instance, at standard conditions the Nernst potential is 1.23 V for water splitting. Practically however, a minimum voltage of 1.6-1.7 V is needed for splitting water due to high activation energies [63-65]. As a comparison at high temperature (>750°C), the Nernst potential is very close to the practical minimum voltage (observed open circuit voltage) for steam splitting [22, 66, 67]. Although the heat demand for electrolysis increases as temperature rises, it only accounts for less than 20% of total energy input [22, 66-68]. Practically, no external heating is needed if the SOECs operate around thermal neutral voltages. If higher yield is required, a cooling loop needs to be included.

As mentioned before, high temperature electrolysis technology has gained significant improvement recently due to the research and development of SOFCs studied by engineers and scientists around the world. The mainstream of HTE research globally has been focused on hydrogen and syngas production, including significant feasibility testing conducted by the Idaho

National Laboratory (INL) [69, 70]. Research has been focused from experimental angles, dealing with single cell tests as well as stack systems evaluation [54, 71]. The European Institute for Energy Research (EIFER) also experimented with HTE of steam, and was able to support steam electrolysis for 1000 to 9000 hours successfully [72]. Polarization resistance degradation of SOEC stacks was found to be related to absorption of feedstock impurities during steam electrolysis and steam/CO_2 co-electrolysis tests [73]. The degradation rate of SOECs during high temperature steam electrolysis (HTSE) was further studied in France by the Alternative Energies and Atomic Energy Commission (CEA). This group designed a more affordable 3-cell stack and reported lower degradation rates than that of similar SOECs [74, 75]. The Institute of Nuclear and New Energy Technology (INET) (based in China) as well as the US Department of Energy's (DOE) Next Generation Nuclear Plant (NGNP) program studied production rates of hydrogen using HTE of steam as part of a system utilizing a High Temperature Gas-cooled Reactor (HTGR) [76, 77]. Another Chinese group, the Ningbo Institute of Materials Technology and Engineering (NIMTE), conducted HTSE tests on a 30-cell stack and was able to optimize the performance of their system to an efficiency of greater than 50% [78, 79]. Research has also been conducted in Korea with researchers at the Korea Institute of Science and Technology studying the regenerative properties of SOFCs [80], and researchers at the Korea Institute of Energy Research studying the effects of different preparation methods on cell performance [81].

A common problem that occurs in high temperature electrolysis is degradation, resulting in shorter cell lifespan and lower efficiency [5, 14]. This led to many high temperature electrolysis experiments determining the ideal material combination for durability improvement. This will be explored in a separate subsection of this chapter. Still, the increased efficiency of

HTE over LTE suggests that the high temperature electrolysis process may be more viable for expanded use in experiments optimizing the SOEC [9].

Compared to the intensive research outcomes of high temperature steam electrolysis to produce hydrogen and steam/CO_2 co-electrolysis to produce syngas, research on CO_2 electrolysis to produce oxygen has only been recently caught up. While all the high temperature electrolysis processes use similar SOECs, their electrochemical pathways are different. An important concern of CO_2 electrolysis is that carbon deposition becomes possible. This is because as the CO_2 reduction reaction progresses and becomes more effective at high temperatures, more CO is produced, resulting in more potential of carbon production from pathway (2) and (3) [82]. Compared to the vast amount of information regarding LTE, carbon deposition of high temperature CO_2 electrolysis has not been fully understood and therefore requires both theoretical and experimental investigations.

In the application discussed in this thesis, a Martian atmospheric carbon dioxide to oxygen converter, the high temperatures required would be realistically provided by harvesting excess heat from an onsite radioisotope thermoelectric generator (RTG) which would also provide the electric power needed for electrolysis. This idea is common in Martian exploration articles, using the nuclear energy already included in the plans to simultaneously power and heat the SOEC [83, 84]. The MOXIE project led by MIT and NASA will operate between 800°C and 850°C, making this experiment, which is modelled from their operating assumptions, even more relevant as a HTE experiment instead of a LTE experiment [8].

2.3 Fuel Composition

Another control variable in electrolysis experiments is the composition of the fuel (gas) mixture entering the cell. Similar to any reaction, the reactant concentrations and operating conditions will directly correlate with the amount and composition of the products. The amount of products refers to the amount of carbon monoxide, oxygen, and carbon solid produced. The primary fuel mixing ratio element pertinent to this investigation is the amount of exhaust gas (CO and CO_2) is recycled back into the fuel mixture since the amount of carbon monoxide at the electrode surface (where the reaction is taking place) has been found to affect the cell performance [12, 36].

Graves *et al.* investigated a fuel mixture of carbon dioxide and methane and found a direct correlation between the mixture ratio and the amount of carbon deposition [85]. Figure 2.1 shows the effects of the different ratios of hydrogen, carbon, and oxygen elements on whether there was any carbon deposition on the electrolysis cell at 600°C. Using that experiment as an example: a reaction that is only reducing carbon dioxide (no methane), where the mole ratio of carbon component to exceed 1/3, carbon deposition is expected [85]. In order for this figure to be useful in the current investigation, only the right line of the triangle can be used, since there will be no hydrogen available to convert carbon dioxide to oxygen on Mars unless it is brought from Earth or harvested from electrolysis of Martian water. This is the same reason that co-electrolysis with water and carbon dioxide, such as that done in [86], is not of primary interest in this investigation, even though it does allow for a slightly broader selection of electrode materials.

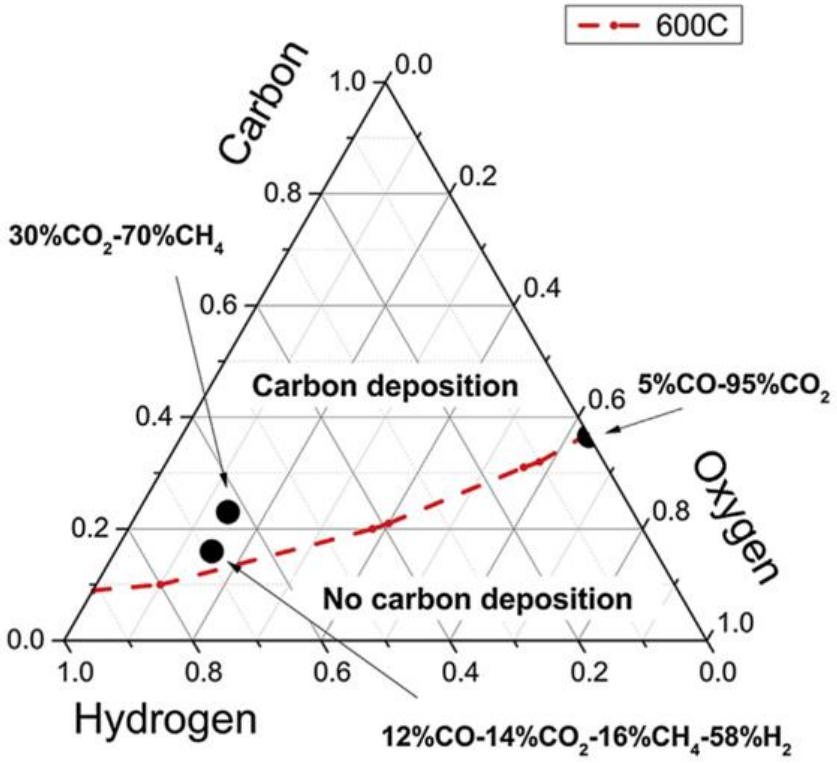

Figure 2.1: Carbon Deposition Limits at 600°C in C-H-O ternary diagram [85].

Recycling the exhaust (a mixture of CO_2 and CO) would ensure a more efficient process as the exhaust would have increasing levels of CO the more recycling occurs. However carbon deposition on the cell seems to be related to the amount of carbon monoxide being produced [12, 36, 82, 85, 87]. A higher proportion of carbon monoxide at the electrode surface (site of the reaction) leads to increased rates of carbon deposition on the electrode. The rate of carbon deposition also increases if carbon monoxide is not properly vented (removed) from the cell to build up concentration over time [87]. The interactions between the gas composition at the electrode and the actual electrode material is an essential consideration if carbon deposition is to

be minimized [85]. Green *et al.* [88] found that there was a decrease in the conductivity and efficiency of the SOEC when the generated carbon monoxide was reintroduced back into the fuel mixture. Again, this is reasonable since more carbon monoxide in the reaction chamber leads logically to a greater chance of solid carbon collecting on the cell. This leads to the third reaction pathway (3) mentioned before where the reduction of carbon monoxide takes place instead of carbon dioxide reduction.

$$CO(g) \rightarrow C(s) + \frac{1}{2} O_2(g) \qquad (3)$$

Both the pathway (2) and (3) could lead to carbon deposition and therefore should be avoided. An important factor in predicting the effect of the fuel mixture on the carbon deposition on the cell is the bond energies, or the energy needed to break the bond. For CO_2 this is 1,598 kJ/mol and for CO is 1,072 kJ/mol [89]. Therefore since the bonding energy for CO_2 is greater than that of CO, it is more likely for CO to break down than CO_2, which would be detrimental since reduction of CO (pathway (3)) leads to carbon deposition. After examining the entirety of each of the chemical reactions (1), (2), and (3) and the bond energies associated with each compound, including O_2 which has a bond energy of 495 kJ/mol and solid carbon which has zero bond energy, the change in bond energy (reactants minus products) is calculated as 279 kJ/mol for pathway (1), 1,103 kJ/mol for pathway (2), and 825 kJ/mol for pathway (3) [89]. This means that, for standard atmospheric temperature and pressure, the preferred path (1) requires less energy than (2) or (3) and is therefore more likely to occur in the SOEC chamber, so long as the excess CO is properly vented and not allowed to build up.

Another concern related to the operation conditions proposed in this thesis, is the potential negative effects due to the other gas impurities directly mixed into the feedstock from the Martian atmosphere, including nitrogen and argon, each of which make up about 1.9% (molar) each of the atmospheric content [2]. Of these two, argon is an inert gas will cause nonhazardous effects throughout the process. A concern might be raised with nitrogen, because nitrous oxide (NO_x) can potentially be produced on the anode where oxygen is evolved. That trace amount of NO_x produced can be eliminated by a filter or absorbent for the purpose of purification of oxygen. On the cathode however, there is a minimum possibility for the production of NO_x due to its reduction environment. Nitrogen will basically act as an inert gas on the cathode. In the real application, both nitrogen and NO_x will not cause any damage to the SOECs as carbon deposition does due to their gaseous states.

2.4 Geometric Setup

2.4.1 Tubular Designs

Tubular configurations can be found in many designs both in SOECs and SOFCs [17, 22, 34, 90]. For example, commercially SOFCs produced by Siemens Westinghouse for large-scale, centralized power generation, are of this shape and design [90]. Tubular designs have a couple advantages. The sealing is much easier with tubular configuration, since it only needs sealant at the ends, which can be placed outside the hot zone. In addition, tubular designs require less complex flow channels for gas distribution, as the tube itself forms a flow channel [22, 59, 91]. However, some major flaws of tubular design have prevented them from being widely used in

industry. Tubular cells are usually expensive to manufacture. Furthermore, interconnects among cells becomes more and more complex as the scale goes up, also resulting in high cost [92].

2.4.2 Planar Designs

Planar designs are much more common and widely used in commercial SOFCs and SOECs. The primary reason for this is the simplicity of the planar electrolysis cell set-up versus the complex shape of the tubular design. As for research, the planar button cell (shown in Figure 2.2) is commonly used. Button cell testing allows for quick assembly and testing of the SOEC, thus making it an ideal geometry for investigating material effects on cell performance, in attempting to improve cell materials and structure [60]. Button cell testing is usually conducted in a tube furnace and requires a relatively high gas flow rate compared to traditionally constructed planar cells [60]. Although this test rig offers economical means for SOEC testing, it is challenging to maintain perfect constant flow and the sealing is sensitive to thermal cycles [23, 40, 49, 93]. One clear indicator of seal failure is instability of the cell voltage [60]. Figure 2.2 shows an example of a test rig being employed for CO_2 electrolysis with a button SOEC on the far end of the tube. Half of the alumina tube connected with the cell is placed in the furnace, with the button cell oriented to be at the center of the furnace, ensuring accurate temperature control. The remaining half section will be exposed to the ambient conditions outside the furnace. The fuel inlet tube (made of 304 stainless steel) is inserted all the way down towards (without contact) the button cell. This will ensure preheating and smooth delivery of the inlet gas. Two wires are attached on each side of the button cell for current collection and voltage detection.

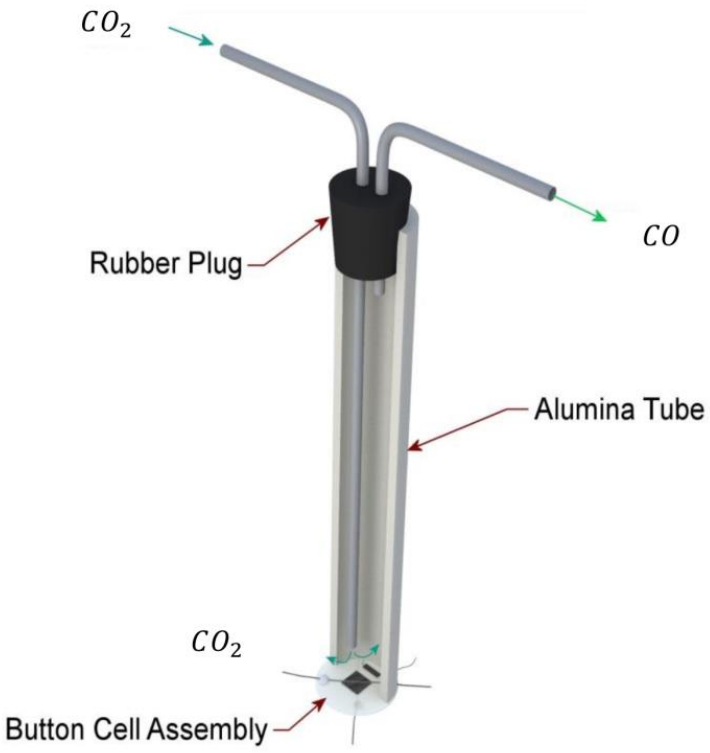

Figure 2.2: Button cell assembly arranged for electrolysis of carbon dioxide.

2.5 Electrolysis Voltage

Another important parameter in SOEC operation is the electrolysis voltage that is applied across the cell. Electrolysis voltage affects the amount of carbon deposition, overall cell performance and reaction efficiency. Electrolysis is a nonspontaneous reaction and therefore requires minimum energy input (i.e. electrical and thermal) to initiate the reaction. Applied electrolysis voltage is directly related to the electrical energy input. The applied voltage also has significant implications for the cell current density, nearly increasing exponentially as the applied voltage to the cell increases [42, 43]. For CO_2 electrolysis at certain temperature, as the voltage varies so will the reactant concentrations across the cell and vice-versa, with oxygen production being directly proportional to the cell voltage [33, 42].

Theoretically the threshold for water electrolysis, or the Nernst potential is calculated via (4) as below [33, 94].

$$V_N = V^0 - \left(\frac{R_U T}{jF}\right) ln\left[\left(\frac{y_{H_2O}}{y_{H_2} y_{O_2}^{1/2}}\right)\right] \quad (4)$$

Equation (4) gives the Nernst potential as a function of the operating temperature (T) and the concentrations chemical species involved in the electrolysis including water, hydrogen, and oxygen $\left(y_{H_2O}, y_{H_2}, \& \, y_{O_2}\right)$. V^0 is the standard cell potential, F is the Faraday constant $\left(F = 96{,}485 \frac{C}{mol}\right)$, and R_U is ideal gas constant $\left(R_U = 8.3145 \frac{J}{mol \cdot K}\right)$. Under different pressures, (4) can be adjusted to the following equation with associated pressure factors [95].

$$V_N = V^0 - \left(\frac{R_U T}{jF}\right) ln\left[\left(\frac{y_{H_2O}}{y_{H_2} y_{O_2}^{1/2}}\right)\left(\frac{P}{P_{std}}\right)^{-1/2}\right] \quad (5)$$

The additional pressure ratio term allows the Nernst Potential to be adjusted for the pressure in the experiment. This will be the equation modified and used in the theoretical chapter of this thesis. Theoretically, as long as the Nernst Potential for (1) is less than that of (2) and (3) and the cell is operated within those parameters, no carbon should form on the cell.

Previous studies have recommended a cell voltage operation range of 0.8 Volts – 2.0 Volts. The minimum voltage of 0.8 V was suggested by Crow *et al.* [40] because no oxygen was produced below that voltage in the experimental and analytical investigations. The maximum voltage of 2.23 V and 2.0 V was suggested by [6, 40] respectively because zirconia might be

reduced and lose its ionic conductivity under those conditions. This detrimental condition was originally discussed in [33]. It is further stated in [6, 96] that if the oxygen pressure on the anode side is allowed to decrease past normal operating conditions, the maximum safe operating voltage would drop to 1.4 V. In order to ensure reliable operation, Crow *et al.* suggested lowering the maximum operating voltage per cell to 1.6 V to avoid the instance where the zirconia starts reduction and breaking down [40].

CO_2 electrolysis needs significant amount of electrical energy input and is the highest power draw in most *in-situ* propellant production system designs [7, 35]. Additionally, oxygen production has been shown to demonstrate a linear relationship with cell current [33]. Since Rapp cited that 12,300 Amperes would be necessary to produce 4 kg/hr of O_2, and the cells were operated in the 1 V – 1.5 V range, a suggested range of power requirement would be 12,300 Watts to 18,450 Watts [5]. In the current plans for Martian oxygen production, electricity as well as heating will come from a nuclear battery, also called RTG. The Viking generators produce approximately 70 W_e but current plans for expansion allow for generators supplying around 120 W_e [83]. There are also designs for 1 kW_e but these approach the size limits (mass wise) of the equipment needed for the mission to Mars [83]. Nevertheless, the nuclear battery needs to be designed to accommodate the large power demand of the electrolysis stack. The heat demand for electrolysis however can be minimized if the stack is operated close to the thermo neutral voltage which makes the electrolysis stack self-sustainable in terms of heating.

2.6 Relation to this Study

The conversion of CO_2 to O_2 using solid oxide electrolysis technology, with the potential application for use on Mars, has been discussed at length. While many studies conducted in

previous years recommended a Reverse Water Gas Shift or Sabatier/water electrolysis system for this use, the need to transport terrestrial hydrogen to Mars in order to support these systems makes them less than ideal [5, 13, 35, 37, 38, 45, 53, 97]. Similarly, water would have to be transported from Earth or harvested from the crust of Mars in order to utilize the benefits of LTE technology for oxygen generation [5, 98]. By contrast, it is much easier to harvest CO_2 from the Martian atmosphere, especially when CO_2 dominates the composition of the Martian atmosphere. High temperature CO_2 electrolysis becomes a more viable technology used for Martial oxygen production. Furthermore, with material and microstructure improvements of SOECs in recent years, including advanced oxygen electrodes (e.g. LSM, LSCM, LSV, and LCC) [17, 48, 51, 86], significant progress has been made on mitigation of SOEC degradation [91]. Recent studies demonstrated extreme long-term durability (close to zero degradation under alternating modes of operation (fuel cell and electrolysis intermittently) [49, 93]. All of those significant advancements make direct CO_2 to O_2 conversion using SOECs more technically ready today for NASA space missions than it was when the idea was conceived. There is a gap, however, in the investigation where the performance of CO_2 electrolysis using SOECs needs to be addressed subjected to the Martian conditions, under which carbon deposition has not been fully understood. This thesis intends to narrow this gap by investigating the operating conditions that can cause detrimental carbon deposition during CO_2 electrolysis using SOECs under Martian conditions.

Chapter 3

Theoretical Analysis

3.1 Theoretical Framework

There are three possible chemical reaction pathways that can occur during the reduction of carbon dioxide in a SOEC. These three pathways are as follows:

$$CO_2\ (g) \rightarrow CO\ (g) + \frac{1}{2}O_2\ (g) + \Delta G_{RXN_1} \quad (1)$$

$$CO_2\ (g) \rightarrow C\ (s) + O_2\ (g) + \Delta G_{RXN_2} \quad (2)$$

$$CO\ (g) \rightarrow C\ (s) + \frac{1}{2}O_2\ (g) + \Delta G_{RXN_3} \quad (3)$$

As indicated, pathways (2) and (3) will lead to solid carbon deposition while (1) is preferred. The Gibbs free energy associated with those three reactions is positive, indicating external energy is needed for the reactions to happen. Each electrochemical reaction has a threshold of minimum electrical energy input, which corresponds directly to its Nernst potential. Therefore, determining the Nernst potential of each pathway at various conditions helps to find an optimal voltage range that is in favor of pathway (1), while minimizing pathways (2) and (3). As a result, this will become a theoretical guideline of the operation of carbon dioxide electrolysis on Mars. For this analysis, the Nernst equation was modified based on equation (5) because it not only allows for the ability to modify and calculate the voltage required based on the composition of the inlet gases but also allows for the experimental pressure to standard pressure ratio to be utilized [95]. This is especially important due to the need to compensate for the lower atmospheric pressure on Mars. In this case though, the particular compounds will be

modified to reflect carbon dioxide reduction instead of water reduction. Thus CO_2 will replace H_2O, CO will replace H_2, and O_2 will remain the same from (5). Each of the variables will be explained and calculated out in detail.

$$V_N = V^0 - \left(\frac{R_U T}{jF}\right) ln\left[\left(\frac{y_{CO_2}}{y_{CO} y_{O_2}^{1/2}}\right)\left(\frac{P}{P_{std}}\right)^{-1/2}\right] \quad (6)$$

This Nernst equation can be modified for the other two pathways. The Nernst potential for pathway (2) can be found via (7) and the Nernst potential for pathway (3) is found via (8).

$$V_N = V^0 - \left(\frac{R_U T}{jF}\right) ln\left[\left(\frac{y_{CO_2}}{y_C y_{O_2}}\right)\left(\frac{P}{P_{std}}\right)^{-1}\right] \quad (7)$$

$$V_N = V^0 - \left(\frac{R_U T}{jF}\right) ln\left[\left(\frac{y_{CO}}{y_C {y_{O_2}}^{1/2}}\right)\left(\frac{P}{P_{std}}\right)^{-1/2}\right] \quad (8)$$

The values held constant in these equations are the Faraday constant $\left(F = 96{,}485 \frac{C}{mol}\right)$, the ideal gas constant $\left(R_U = 8.3145 \frac{J}{mol \cdot K}\right)$, and the ratio of atmospheric pressures between Mars and Earth. The experimental pressure *P* is of utmost importance in this analysis, as the atmospheric pressure of Mars is 0.5683% of Earth's, though the pressure of Mars fluctuates at about a 30% range over the course of a Martian day [1, 2, 40]. For calculations of Equations (6), (7), and (8), the ratio of experimental pressure *P* to standard terrestrial atmospheric conditions P_{std} is then considered to be: $\frac{P}{P_{std}} = 0.005683$. As mentioned in Section 2.5, the major variables of concern are operating temperature (T) and the concentrations of the substances at the

electrodes $(y_{CO_2}, y_{CO}, \& \, y_{O_2})$. For this experiment, the concentrations of each substance is equivalent to the partial pressure of that component and will be evaluated as independent variables later as the inlet gas composition ratio has been shown in research to greatly affect the Nernst potential of the reaction [12, 82, 85, 87, 88]. For (2) and (3), where solid carbon is present, it is necessary to assume the concentration to be equal to 1 ($y_C = 1$). While the CO_2, O_2, and CO terms are gases and the partial pressure of each gas can be used to represent its concentration, solids such as carbon are solids and therefore their concentration is considered 1 in electrochemical calculations [99, 100].

The nitrogen to NO_X reaction mentioned in Section 2.3 would only occur in the anode chamber for this setup and is not part of the electrolysis reaction that is studied here and modeled in the Nernst potential equations. Because of this, any NO_X conversion that would occur would have a limited effect on the Nernst equation; only minor fluctuations in the partial pressures of the gases would be observed.

The Nernst potential at standard conditions, V^0, in (6), (7), and (8) can be calculated using (9), shown below [62]. It is the relation of Gibbs free energy change divided by the mole number of electrons transferred in the reaction and Faraday's constant [62]. The Gibbs Free Energy function is given in (10) and is dependent on the enthalpy (h) and entropy (s) of each of the elements of the reaction [62].

$$V^0 = -\frac{\Delta G_{RXN}}{jF} \tag{9}$$

$$\Delta G_{RXN} = \Delta H_{RXN} - T\Delta S_{RXN} \tag{10}$$

The Gibbs Free Energy of each of the chemical reactions at different temperatures was obtained from the website [101]. Using the Gibbs energy of the entire reactions instead of for each of the components is necessary in order to increase the accuracy of the value, since the reaction is being looked at as a whole. These values, per reaction, per temperature can be found below in Table 3.1.

Table 3.1: Gibbs free energy values for chemical reactions (1), (2), & (3) for the temperature range room temperature - 1200 K [101].

T (K)	298	400	500	600	700	800	900	1000	1200
ΔG_{RXN_1} (kJ/mol)	257.2	248.4	239.7	231.1	222.4	213.8	205.1	196.5	179.2
ΔG_{RXN_2} (kJ/mol)	394.4	394.7	394.9	395.2	395.5	395.8	396.1	396.4	396.9
ΔG_{RXN_3} (kJ/mol)	137.2	146.3	155.2	164.1	173.1	182.0	191.0	199.9	217.8

Thus (6) and the Nernst potential, or theoretical minimum electrolysis voltage necessary to drive nonspontaneous reactions, was calculated for various inlet gas compositions (by manipulating the partial pressures) and temperatures of interest.

3.2 Results

Simulations were conducted using a code written and executed in Matlab (Math Works, Natlick, MA), which is provided in Appendix 1. Once the Nernst potential was corrected for pressure and inlet composition to give the fully evaluated values, the results of the three plotted equations can be compared to each other in order to determine the optimal operating voltages

that minimize carbon deposition and thus cell damage. In theory, a safe zone of operation is expected to sustain pathway (1) while constraining pathways (2) and (3).

The results of the simulation are illustrated in Figures 3.1 – 3.5. The figures demonstrate the Nernst potentials of three electrolysis pathways with various gas concentrations and temperatures under the Martian atmospheric pressure. In the cases shown in the figures, inlet gas compositions of pure CO_2 (Figure 3.1), 90% CO_2 + 10% CO (Figure 3.2), 70% CO_2 + 30% CO (Figure 3.3), 50% CO_2 + 50% CO (Figure 3.4), and 30% CO_2 + 70% CO (Figure 3.5) were used. Those cases are selected to simulate the gas concentrations at different locations of SOEC stack during electrolysis. A different satisfactory minimum temperature is associated with each inlet composition of the SOEC. The acceptable minimum temperature and the maximum voltage to avoid carbon deposition at that temperature for each inlet gas composition, based on graphical interpretation, are displayed below in Table 3.2.

Table 3.2: Threshold to avoid carbon deposition (analysis from Figures 3.2-3.5).

Gas Composition (%)		Min.	Max. Applicable Voltage (V)			
CO_2	**CO**	**Temp.(°C)**	**800 °C**	**900 °C**	**1000 °C**	**1100 °C**
90	10	980	N/A	N/A	1.21	1.23
70	30	810	N/A	1.19	1.21	1.22
50	50	750	1.17	1.18	1.20	1.21
30	70	690	1.16	1.17	1.18	1.19

As seen in Figures 3.1 – 3.5, each inlet composition has its own “Safe Zone of Operation” that has a low likelihood of carbon deposition. This “Safe Zone of Operation” is created as the Nernst potential is able to sustain reaction (1) while constraining reactions (2) and

(3). That means the cell voltage is high enough to drive the reaction (1), but not high enough to drive the other two reactions that result in carbon deposition. Thus, each safe zone is shaped by a minimum temperature and a minimum and maximum voltage. So long as operation is maintained in these temperature ranges and at the required voltage, the SOEC will operate successfully with minimum carbon deposition and subsequent cell degradation.

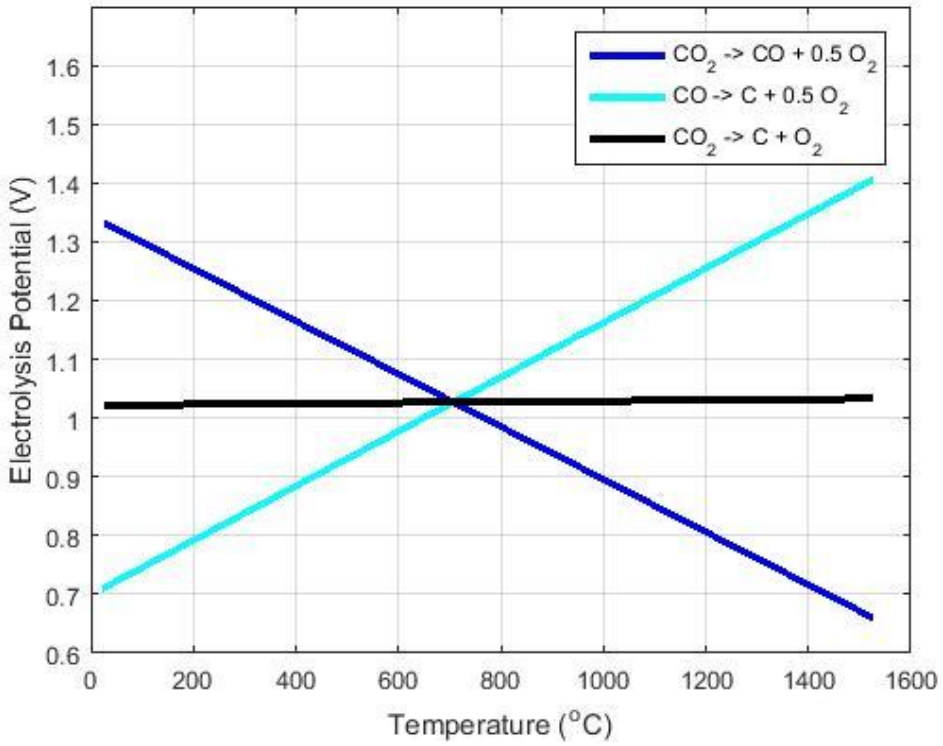

Figure 3.1: Nernst potentials of three electrolysis pathways under Martian atmosphere.

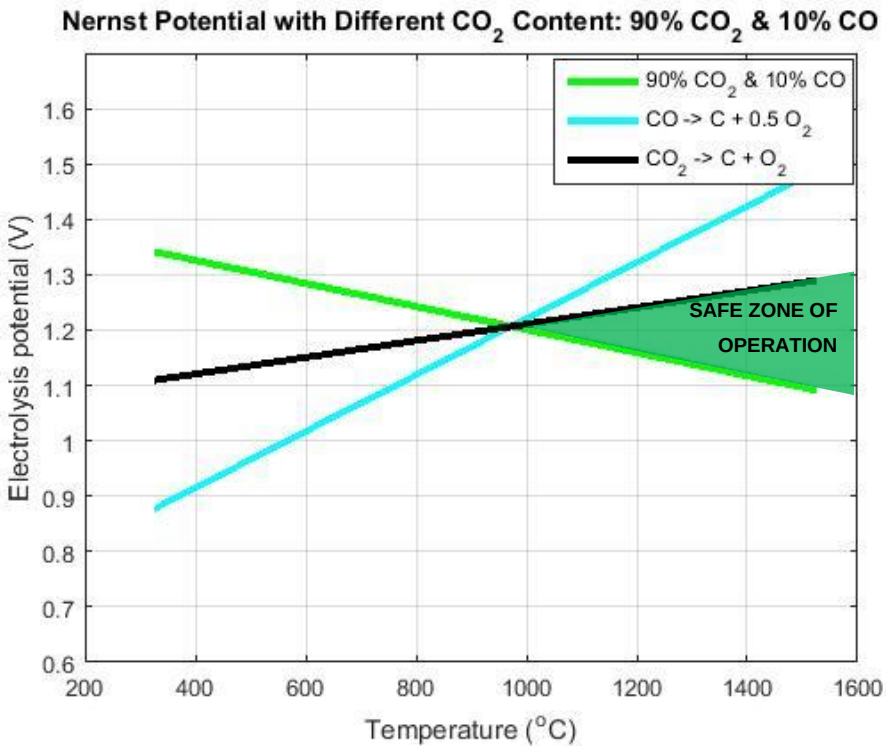

Figure 3.2: Nernst potential for the gas inlet composition 90% CO_2 + 10% CO. The green zone shows the voltages that can sustain oxygen production while minimizing hazardous carbon deposition.

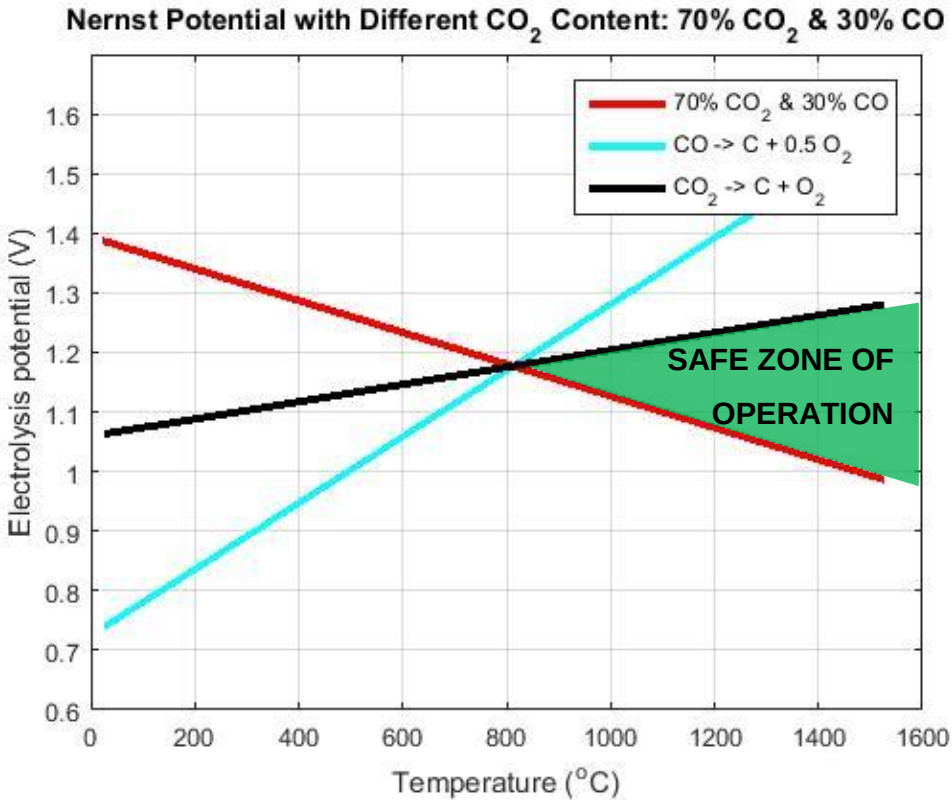

Figure 3.3: Nernst potential for the gas inlet composition 70% CO_2 + 30% CO.

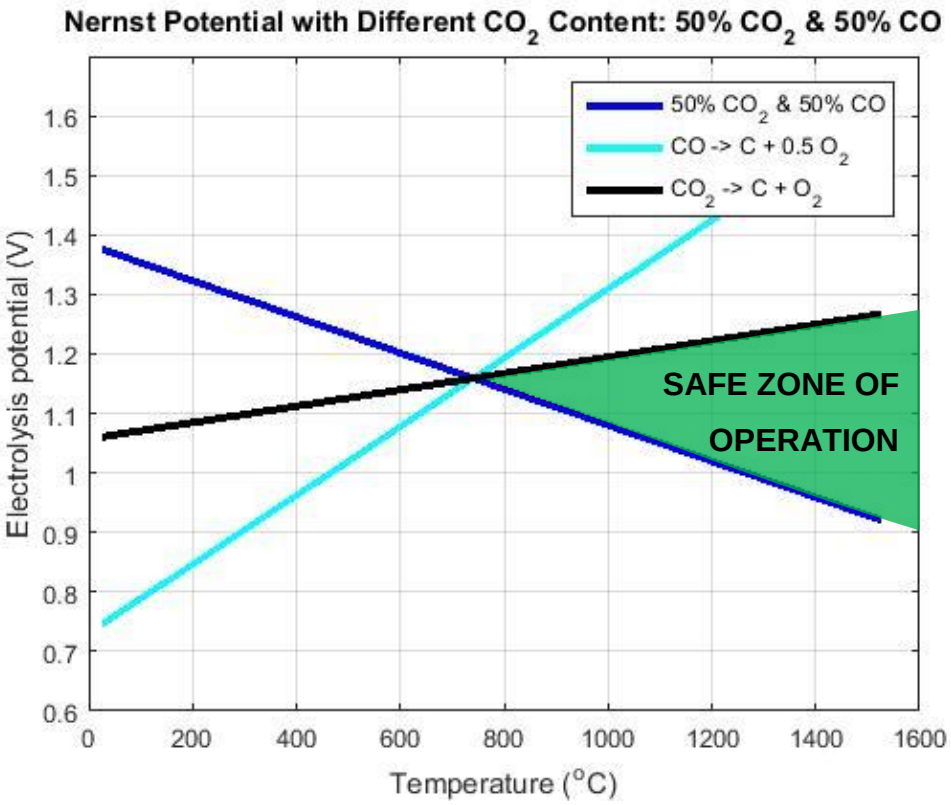

Figure 3.4: Nernst potential for the gas inlet composition 50% CO_2 + 50% CO.

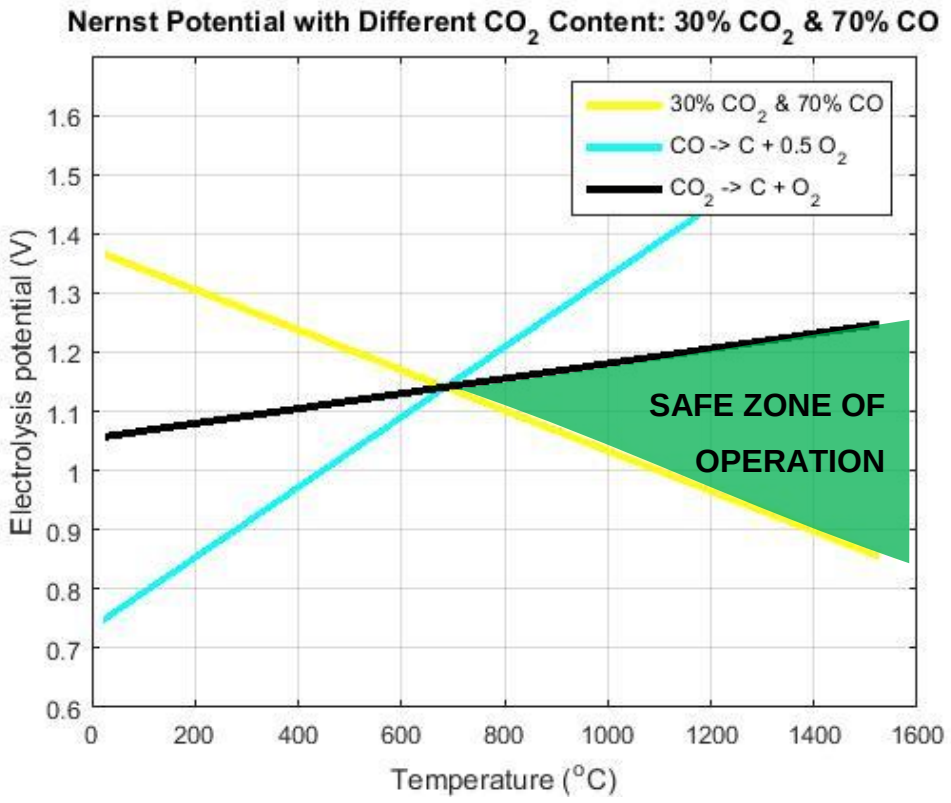

Figure 3.5: Nernst potential for the gas inlet composition 30% CO2 + 70% CO.

Chapter 4

Preliminary Experimental Results

4.1 SOEC Button Cell Preparation

The objective of the experimental research is to evaluate and validate the prediction of "Safe Zone of Operation" in Chapter 3. Although SOECs are available commercially, the common use of nickel as a catalyst prevented their use in this study as nickel can be easily oxidized during CO_2 reduction. As stated earlier, button cell geometry was selected due to its relative simplicity and aptitude for testing of this nature. A full schematic for the entire button cell assembly can be seen below in Figure 4.1.

Because of the need for accurate measurement of the active cell area, the construction of the SOEC started with cutting two silver mesh squares, each with an area of 1 cm^2. This would allow for accurate current density calculations. A mask with a square opening was used to ensure accurate application of the electrode materials on the substrates. The composite electrodes were prepared using the mixture of silver and Yttria Stabilized Zirconia (YSZ) using the weight ratio of 1:1 [42, 43]. Silver works as the anode catalyst for oxygen evolution and also as the cathode catalyst for fuel. Mixing YSZ into the electrode helps to increase the active areas of triple phase boundary of electrode/electrolyte. For the preparation process, first, 0.5 grams of silver paste was added to a small beaker. Then, YSZ powder was added to a separate tray. The mass of this powder was 70% of the mass of the silver paste since the silver paste was 70% silver by mass. Compensating for this ensured that the weight ratio of silver and YSZ was 1:1. The YSZ was added to the small beaker of silver paste. In order to break down the silver paste and

allow for proper and uniform bonding between the YSZ and the silver, 100 ml of Xylene was added. The solution was mixed lightly with forceps.

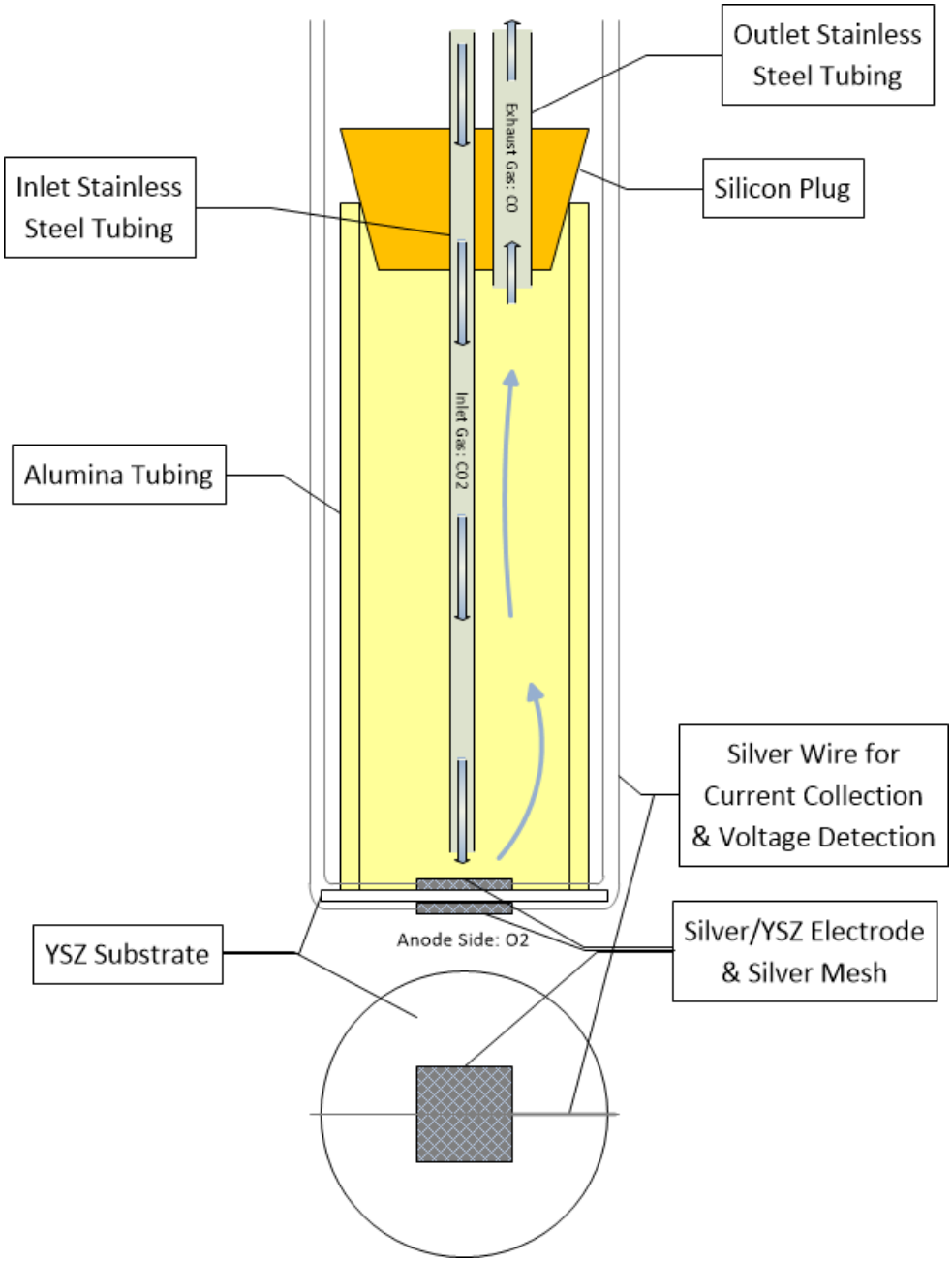

Figure 4.1: Cell assembly schematic.

The solution was then placed on the magnetic mixer plate. An appropriately sized magnetic stirrer was added to the small beaker and the magnetic mixer was set to 100°C and 1200 revolutions-per-minute. The solution was allowed to mix for approximately 45 minutes, or until the YSZ/Silver Paste thickened.

Once the electrolyte silver-YSZ paste was ready, tape was applied to one side of the YSZ 32 mm substrate, leaving only a square-shaped 1 cm^2 area in the center of the substrate for the silver mesh and electrolyte paste. The paste was applied to the top of the YSZ substrate within the taped off square and the silver mesh was placed into the silver paste applied to the substrate so that it was imbedded within the paste. Similarly, silver wire, for current collection, was adhered to the substrate surface using the silver paste and the entire YSZ substrate was sintered in the furnace with the maximum heating temperature of 800°C for one hour. During the heating and cooling process getting to 800°C from room temperature and coming down from 800°C to room temperature, the temperature was increased and decreased at the rate of 2°C per minute.

Additionally, some cells were constructed with all silver electrodes, thus eliminating the mixture of the YSZ powder into the silver paste. This was due to poor cell performance in initial tests, thought to be the result of electrodes that were too thick and not porous enough for gases. The silver paste was applied directly to the YSZ 32 mm substrate and the 1 cm^2 silver mesh was imbedded into the paste. These cells were heated at 100°C for one hour before the silver wire was added and the whole button cell was sintered in the furnace at 800°C for one hour, with increasing and decreasing rates of 2°C per minute. The button cell discussed here is shown in Figure 4.2.

An alumina tube was used to control the inlet and outlet gases on the anode side of the button cell. To prepare the tube for the button cell, notches were created across the diameter of

the tube on one side. This allowed for the silver wire on the anode side (sealed off from the outside) to pass through the alumina tube so that current be collected. After the button cell was prepared, it was adhered to the alumina tube using ceramic glue (Cermabond 522 by Aremco Products, Inc.) with the silver wires on the anode side passing through the notches mentioned earlier. These notches were then sealed with ceramic glue to eliminate any leakage. Longer pieces of silver wire (used for current collection), shielded in insulation, were adhered to the silver wire strips already attached to the button cell using ceramic glue and were taped to the side of the alumina tube.

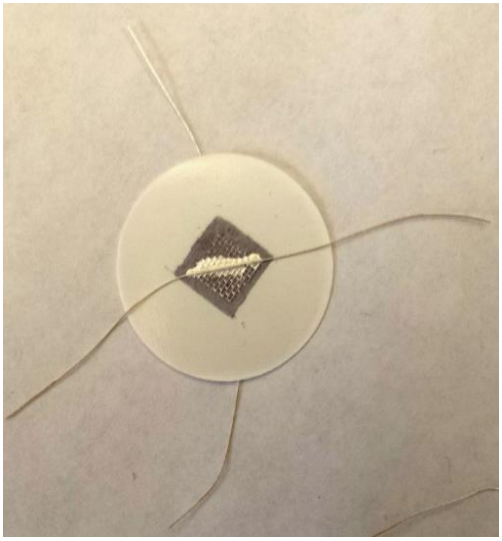

Figure 4.2: Surface of the button cell with the YSZ substrate, silver paste electrode and silver wire and mesh for current collection.

Two holes were drilled through a rubber plug which was fitted into the opposite end of the alumina tube, allowing gas feeding and venting. The inlet stainless steel tube was inserted in

one hole all the way down to the cell to ensure maximum fuel contact with the electrode. The outlet tube was shorter, nearer the plug, to ensure smooth venting. The alumina tube with button cell attached is visible in Figure 4.3.

Figure 4.3: Alumina tube used for button cell testing with wires for current collection running along the outside and the button cell at one end.

A clamp held the alumina tube in the horizontal tubular furnace and the gas inlet, gas outlet, and silver wires were connected to a solid oxide fuel cell test stand (Scribner 855 SOFC). This setup is visible in Figure 4.4.

The single button cell fabrication process can be viewed graphically on the next page (Figure 4.5).

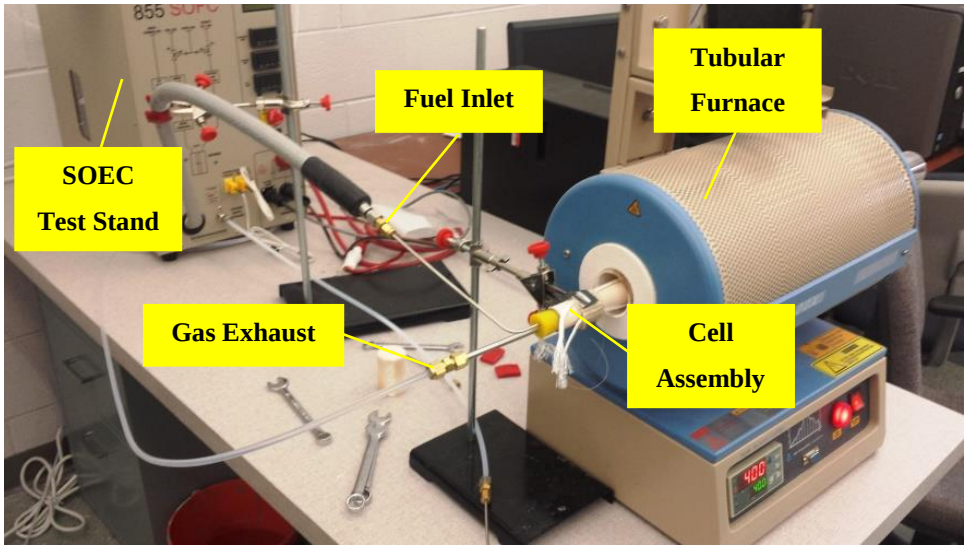

Figure 4.4: SOEC Testing Station and tubular furnace.

Figure 4.5: Cell assembly construction procedure.

4.2 Experimental Design

The experiments were designed to first test the button cell in the fuel cell mode using hydrogen gas and then test the cell's ability to pump oxygen ions in the electrolysis mode. During oxygen pump mode testing, oxygen ions were moved through the electrolyte in the same direction that they would under actual CO_2 reduction conditions, thus making oxygen pump mode testing a necessary step in ensuring proper cell function. Following successful testing, the cell can be used for CO_2 electrolysis tests. To simulate the Martian atmosphere, a specialty gas mixture was purchased from Airgas. The gas mixture consists of 0.6% CO_2 balanced with nitrogen gas in order to simulate CO_2 partial pressure on Mars. This was a favorable method for reducing the pressure of CO_2 instead of a vacuum pump design since it allowed to use of the existing SOEC test stand without modification. Electrolysis testing of the button cell and then observation of the carbon deposited on the cell surface will then occur to verify the generated model and determine experimental conditions that will minimize carbon deposition.

4.3 Preliminary Experimental Results

Thus far there have been two series of preliminary tests conducted on the SOECs fabricated from the procedure described above. The first test was to operate the cell in fuel cell mode with hydrogen gas at 500 sccm fueling the cell's reaction, resulting in a $H_2\,(g) + \frac{1}{2}O_2\,(g) \rightarrow H_2O\,(g)$ reaction and producing electricity. The cell operating temperature was kept at 750°C and the open circuit cell voltages were measured. The operating temperature was selected based on the results of Chapter 3. The button cell in this experiment was able to maintain an open voltage of about 0.86 Volts (V) for three hours before the heat caused the ceramic glue adhering the silver wire to the Monel wire to fail and the wires to detach.

The second test was designed to ensure that the cell works in the fuel cell mode, as well as to determine if the second SOEC would produce a higher open circuit voltage (OCV) than the first one. The cell operated under the same conditions as the first did (500 sccm hydrogen fuel and 750°C) and generated a maximum OCV of about 0.93 Volts but failed to produce any significant current. Once the cell was inspected upon cooling, it was found that the Monel wire was oxidized in the high temperature conditions, thereby increasing resistance to the point where electrical current was undetectable.

After the first two tests, the Monel wiring was replaced with silver wiring. Another modification was the tube furnace was reoriented from the horizontal to the vertical position for better hydrogen gas feeding. A third hydrogen based fuel cell test of the button cell was conducted and this cell reached a peak OCV of 0.91 Volts but only small current was carried on the silver wires. That indicates other resistance, rather than Ohmic resistance, was too high. It was speculated that the electrodes were not porous enough such that the gas diffusion resistance was too high.

To increase the porosity of the electrode, the fourth button cell was prepared with all silver electrodes. This cell was tested using a similar procedure to the first three and was found to carry current. Modifying the electrode mixture to a solely silver based composition helped to improve cell construction success likelihood as the mixing of the silver paste and YSZ powder using Xylene would not always yield operable cells after the sintering process. About one-third to half of the fabricated button cells with the silver-YSZ electrodes were found to have cracked electrodes that would not adhere to the YSZ substrate after removal from the furnace. In order to prove that the SOEC was functioning properly and able to conduct oxide ions, the cell was next

tested in oxygen pump mode and its performance is displayed graphically below in Figure 4.6 (raw data for this experiment can be found in Appendix 2: Oxygen Pump Mode Data).

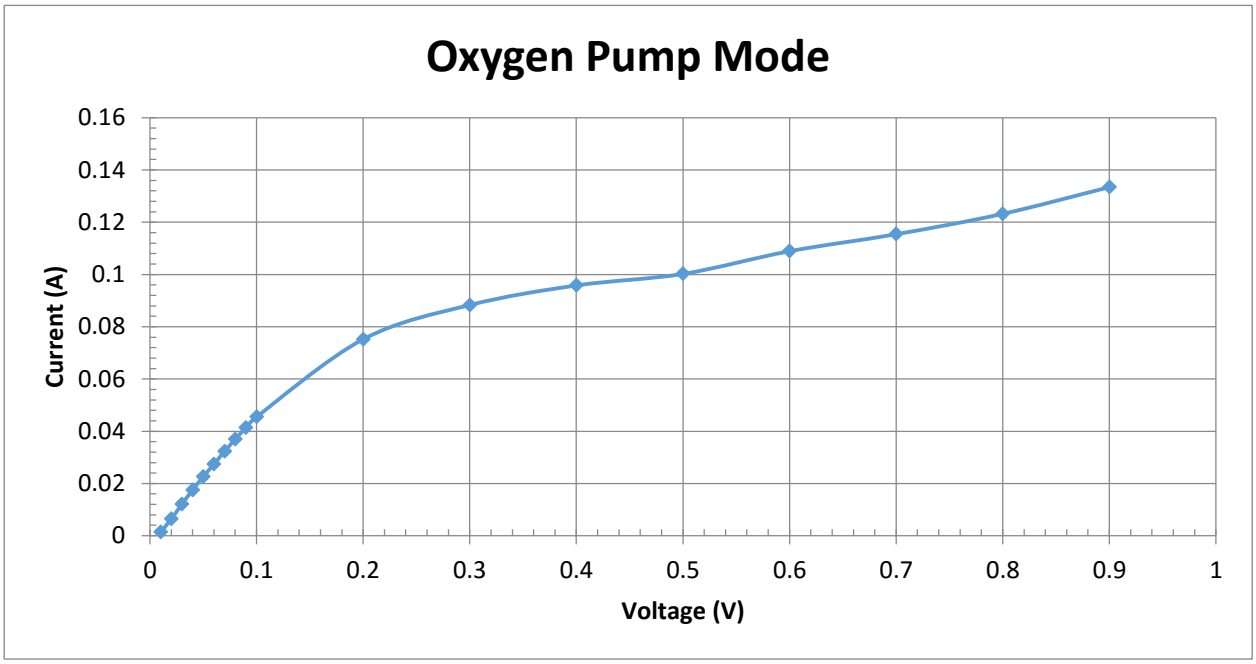

Figure 4.6: Performance of the SOEC in oxygen pump mode.

As seen in Figure 4.6, there are two regions of performance for the solid oxide button cell in oxygen pump mode. The first region (from 0.01 V – 0.1 V) demonstrates a linear relationship between current and voltage, while the second region (greater than 0.1 V) demonstrates a more converging relationship at first and then begins increasing again as voltages increase. When the oxygen consumption rate is less than its supply, the V-I curve demonstrated linear characteristics (as shown in Figure 4.6 where voltage is lower than 0.1 V), since the overpotentials at such

conditions are minimum at high temperature. As the current increased and oxygen demand surpassed supply, the cell became starving and the electrode overpotentials started to build up. This was mainly caused by limited porosity of the electrodes.

Unfortunately, the experimental investigation has only been carried so far in this thesis due to limited funding and lab materials. As seen in Table 4.1, the total estimated cost of this research was $1,307.78. This does not include the cost of lab materials (measurement instruments, magnetic mixer, test stand) and fuel (hydrogen or CO_2). In order to continue with experimental verification of the proposed model, additional funding must be provided.

Table 4.1: Estimated cost for this research.

Material	Vendor	Estimated Cost
YSZ Substrates	Fuel Cell Materials	$225.00
YSZ Powder	Fuel Cell Materials	$185.00
Silver Paste	Fuel Cell Materials	$95.00
Silver Mesh	Fuel Cell Materials	$205.00
Silver Wire	Fisher Sci.	$291.23
Monel Wire	MWS Wire Industries	$130.00
Silicon Plugs	Stockcap	$46.55
Stainless Steel Tubing	McMaster-Carr	$40.00
Alumina Tubing	McMaster-Carr	$90.00
TOTAL ESTIMATED COST		**$1307.78**

Chapter 5

Conclusions and Future Work

5.1 Conclusions

The goal of this project was to investigate the conditions at which carbon deposition would occur during carbon dioxide electrolysis to produce oxygen using SOECs. This was investigated in order to determine the potential for space exploration application as a conversion system to convert carbon dioxide to oxygen on Mars, under Martian atmospheric conditions. The experimental investigation is underway with the theoretical analysis completed in this thesis.

The fuel cell theory and thermodynamics were used to determine the Nernst potential of different oxygen generation pathways at Martian conditions with different gas compositions in the feedstock. The "Safe Zone of Operation", simulating four different fuel composition ratios, for oxygen production on Mars was predicted. This encompassed a range of operating electrolysis voltages and temperatures under which certain fuel inlet mixtures would produce minimal carbon deposition. As the CO_2 concentration decreases in the feedstock (fuel composition ratio), the minimum temperature needed for safe operation is lowered. This gives a smaller "Safe Zone of Operation" though, meaning there is a smaller range of cell voltage to safely operate within. Thus, it is suggested that cell performance is probably optimized at CO_2 concentrations less than 70% but at temperatures greater than 800°C. The CO_2 concentrations can be lowered by recycling CO back into the feedstock. This model can be used as a guideline of oxygen production using SOECs at Martian atmospheric pressure.

This thesis aimed to provide theoretical ranges at which SOECs would be able to safely operate in converting CO_2 to O_2 in a Martian environment. The findings can be used to guide the

continuing experimental investigation in the future, using the SOECs constructed as part of this study's parallel investigation.

5.2 Future Work

If additional funding can be provided, the experimental investigation would be allowed to continue. The experimental investigation is needed to validate the model and verify the safe zones of operation predicted by the model.

With the needed funding, the experimental investigation can be continued using electrolysis to reduce CO_2 using the fuel mixture of CO_2 balanced with nitrogen to simulate the Martian atmospheric pressure. Using this fuel supply and constructing a double ended Alumina button cell testing tube would allow for accurate, Martian atmosphere simulating experiments. The experimental efficiency of the process under Martian conditions can be determined from the results of this experiment. Additionally, the button cell can be placed under a microscope and the amount of carbon deposition can be recorded measured in units of surface area and thickness as well as weight by weighing the cell before and after the experiment. However, the simulated Martian environment may not be the actual one used for Martian oxygen production in the MOXIE project. For the MOXIE application, CO_2 will be compressed before feeding into the SOECs to minimize gas diffusion resistance due to the low Martian atmosphere pressure. Experimental accuracy can be increased with better equipment to prepare the electrodes accurately (e.g. tape casting, screen printing, chemical vapor deposition), but this would require a great deal of funding which was not available at the time of this study.

Once there is successful operation of the CO_2 electrolysis process, it will be possible to optimize the experiment using a statistically designed experiment. In this process the effects of

the factors of interest (variables that can be manipulated) on the response variable are quantified and an experimental model is generated to predict the response given values for each of the factors of interest. If this study was examined as a statistically designed experiment, the factors of interest would be the electrolysis voltage across the SOEC, the gas inlet mixture (CO_2 to CO ratio), and the operating temperature. The response would be the amount of carbon deposited on the cell. Lastly, the pressure of the experiment would be held constant. Since this is a three factor experiment, a 2^3 factorial investigation would be set up. Center points (points within the minimum and maximum values for the factors of interest) would be recommended in order to increase model accuracy and help with full comprehension of factor effects. Additionally duplicates are recommended as these would further strengthen the model. Generally in a statistically designed experiment, each factor level would be randomized. Thus the trial runs would have prescribed, randomized factor settings. In theory this eliminates any experimental noise that could have adverse effects on the accuracy of the data. For this experiment, however, it is recommended not to randomize due to the buildup of gasses within the SOEC. Based on previous experience, this gas buildup can cause misleading data to be collected especially if a lower fuel flow rate is considered after a high fuel flow rate. Using the model generated via an analysis of variance, the operation of the SOEC could be optimized to minimize carbon deposition and ideal variable settings could be determined. It is suggested that for the design of experiments portion of the investigation, Design-Expert (Stat-Ease, Inc., Minneapolis, MN) be utilized for ease of analysis of variance calculations.

Works Cited

[1] D. R. Williams. (2013, 1/30/2015). *Earth Fact Sheet* [Electronic]. Available: http://nssdc.gsfc.nasa.gov/planetary/factsheet/earthfact.html

[2] P. R. Mahaffy, C. R. Webster, S. K. Atreya, H. Franz, M. Wong, P. G. Conrad, *et al.*, "Abundance and Isotopic Composition of Gases in the Martian Atmosphere from the Curiosity Rover," *Science*, vol. 341, pp. 263-266, July 19, 2013 2013.

[3] K. Maxey. (2014, 01/30/2015). Can Oxygen Be Produced on Mars? MOXIE Will Find Out. Available: http://www.engineering.com/DesignerEdge/DesignerEdgeArticles/ArticleID/8200/Can-Oxygen-Be-Produced-on-Mars-MOXIE-Will-Find-Out.aspx

[4] W. Maia. (2014, 01/30/2015). Going to the Red Planet. *MIT News*. Available: http://newsoffice.mit.edu/2014/going-red-planet

[5] D. Rapp, *Human Missions to Mars: Enabling Technologies for Exploring the Red Planet*. Heidelberg, New York: Springer-Praxis Books in Astronautical Engineering, 2008.

[6] S. P. Brod, "A testbed for investigating the effect of electrode structure on the performance of a solid oxide electrolysis system," 1995.

[7] M. Stancati, J. Niehoff, W. Wells, and R. Ash, "Remote Automated Propellant Production: A New Potential for Round Trip Spacecraft," *AIAA Paper*, pp. 79-0906, 1979.

[8] J. A. H. Michael H. Hecht, MOXIE Team, "The Mars Oxygen ISRU Experiment (MOXIE) on the Mars 2020 Rover," presented at the 46th Lunar and Planetary Science Conference (2015), 2015.

[9] U. Sunghyun and K. Young Dok, "Electrochemical conversion of carbon dioxide in a solid oxide electrolysis cell," *Current Applied Physics*, vol. 14, pp. 672-9, 05/ 2014.

[10] W. Li, Y. Shi, Y. Luo, Y. Wang, and N. Cai, "Carbon deposition on patterned nickel/yttria stabilized zirconia electrodes for solid oxide fuel cell/solid oxide electrolysis cell modes," *Journal of Power Sources*, vol. 276, pp. 26-31, 2015.

[11] T. Youkun, S. D. Ebbesen, and M. B. Mogensen, "Carbon Deposition in Solid Oxide Cells during Co-electrolysis of H2O and CO2," *Journal of the Electrochemical Society*, vol. 161, pp. 337-43, / 2014.

[12] S. D. Ebbesen and M. Mogensen, "Electrolysis of carbon dioxide in Solid Oxide Electrolysis Cells," *Journal of Power Sources*, vol. 193, pp. 349-358, 2009.

[13] L. Wenying, S. Yixiang, L. Yu, and C. Ningsheng, "Elementary reaction modeling of solid oxide electrolysis cells: Main zones for heterogeneous chemical/electrochemical reactions," *Journal of Power Sources*, vol. 273, pp. 1-13, 01/01 2015.

[14] R. N. Singh, "High-temperature seals for solid oxide fuel cells (SOFC)," *Journal of Materials Engineering and Performance*, vol. 15, pp. 422-6, 08/ 2006.

[15] A. L. Dipu, J. Ryu, and Y. Kato, "Carbon dioxide electrolysis for a carbon-recycling iron-making system," *ISIJ International*, vol. 52, pp. 1427-1432, 2012.

[16] A. L. Dipu, Y. Ujisawa, J. Ryu, and Y. Kato, "Carbon dioxide reduction in a tubular solid oxide electrolysis cell for a carbon recycling energy system," *Nuclear Engineering and Design*, vol. 271, pp. 30-35, 2014.

[17] D. Clark, R. Losey, and J. Suitor, "Separation of oxygen by using zirconia solid electrolyte membranes," *Gas separation & purification*, vol. 6, pp. 201-205, 1992.

[18] W. Doenitz, R. Schmidberger, E. Steinheil, and R. Streicher, "Hydrogen production by high temperature electrolysis of water vapour," *International Journal of Hydrogen Energy,* vol. 5, pp. 55-63, 1980.

[19] W. Doenitz and R. Schmidberger, "Concepts and design for scaling up high temperature water vapour electrolysis," *International Journal of Hydrogen Energy,* vol. 7, pp. 321-330, 1982.

[20] W. Doenitz and E. Erdle, "High-temperature electrolysis of water vapor—status of development and perspectives for application," *International Journal of Hydrogen Energy,* vol. 10, pp. 291-295, 1985.

[21] W. Doenitz, G. Dietrich, E. Erdle, and R. Streicher, "Electrochemical high temperature technology for hydrogen production or direct electricity generation," *International journal of hydrogen energy,* vol. 13, pp. 283-287, 1988.

[22] M. A. Laguna-Bercero, "Recent advances in high temperature electrolysis using solid oxide fuel cells: a review," *Journal of Power Sources,* vol. 203, pp. 4-16, 04/01 2012.

[23] S. M. Hashim, A. R. Mohamed, and S. Bhatia, "Current status of ceramic-based membranes for oxygen separation from air," *Advances in Colloid and interface Science,* vol. 160, pp. 88-100, 2010.

[24] M. Jitaru, "Electrochemical carbon dioxide reduction-fundamental and applied topics," *Journal of the University of chemical Technology and Metallurgy,* vol. 42, pp. 333-344, 2007.

[25] P. A. Lessing, "A review of sealing technologies applicable to solid oxide electrolysis cells," *Journal of Materials Science,* vol. 42, pp. 3465-3476, 2007.

[26] D. D. Gross. (2010, Sept/Oct 2010) Fuel Cells: 170 Years of Technology Development - and Space Age Experience! *Fuel Cell Special*. Available: http://www.cleantechinvestor.com/portal/fuel-cells/6455-fuel-cell-history.html

[27] P. L. Barry. (2000, 4/10/16). *Breathing Easy on the Space Station*. Available: http://science.nasa.gov/science-news/science-at-nasa/2000/ast13nov_1/

[28] J. Fitzgerald and N. O'Bryan. (2005). *Fuel Cells: A Better Energy Source for Earth and Space*. Available: http://www.nasa.gov/centers/glenn/technology/fuel_cells.html

[29] B. Dunbar. (2010). *Summary: Space Applications of Hydrogen and Fuel Cells*. Available: http://www.nasa.gov/topics/technology/hydrogen/hydrogen_2009.html

[30] C. Iacomini, "Demonstration of a stand-alone solid oxide electrolysis stack with embedded sabatier reactors for 100% oxygen regeneration," in *41st International Conference on Environmental Systems, AIAA*, 2011.

[31] R. Ash, W. Dowler, and G. Varsi, "Feasibility of rocket propellant production on Mars," *Acta Astronautica*, vol. 5, pp. 705-724, 1978.

[32] A. C. Muscatello and E. Santiago-Maldonado, "Mars in situ resource utilization technology evaluation," in *50th AIAA Aerospace Sciences Meeting*, Nashville, Tennessee, 2012.

[33] R. Richter, "Basic Investigation into the Production of Oxygen in a Solid Electrolyte Process," presented at the AIAA 16th Thermophysics Conference, Palo Alto, CA, 1981.

[34] R. L. Ash, M. B. Haywood, and J. A. Werne, "Design of a Mars oxygen processor," *The case for Mars III: Strategies for exploration- Technical(A 90- 16526 04-12). San Diego, CA, Univelt, Inc., 1989*, pp. 479-487, 1989.

[35] R. H. Frisbee, J. R. French Jr, and E. A. Lawton, "A new look at oxygen production on Mars-In situ propellant production (ISPP)," 1987.

[36] R. Zubrin, B. Frankie, and T. Kito, "Mars In-Situ Resource Utilization Based on the Reverse Water Gas Shift: Experiments and Mission Applications," *AIAA Paper*, pp. 97-2767, 1997.

[37] K. Sridhar, J. Finn, and M. Kliss, "In-situ resource utilization technologies for Mars life support systems," *Advances in Space Research*, vol. 25, pp. 249-255, 2000.

[38] K. Sridhar, C. S. Iacomini, and J. E. Finn, "Combined H2O/CO2 solid oxide electrolysis for mars in situ resource utilization," *Journal of propulsion and power*, vol. 20, pp. 892-901, 2004.

[39] K. Sridhar and B. Vaniman, "Oxygen production on Mars using solid oxide electrolysis," *Solid State Ionics*, vol. 93, pp. 321-328, 1997.

[40] S. C. Crow, "The MOXCE Project- New cells for producing oxygen on Mars," in *AIAA/ASME/SAE/ASEE Joint Propulsion Conference & Exhibit, 33 rd, Seattle, WA*, 1997.

[41] D. L. Clark, "In-situ propellant production on Mars: A Sabatier/electrolysis demonstration plant," in *Situ Resource Utilization (ISRU) Technical Interchange Meeting, February*, 1997, pp. 4-5.

[42] G. Tao, K. R. Sridhar, and C. L. Chan, "Study of carbon dioxide electrolysis at electrode/electrolyte interface: Part I. Pt/YSZ interface," *Solid State Ionics*, vol. 175, pp. 615-619, 11/30/ 2004.

[43] G. Tao, K. R. Sridhar, and C. L. Chan, "Study of carbon dioxide electrolysis at electrode/electrolyte interface: Part II. Pt-YSZ cermet/YSZ interface," *Solid State Ionics,* vol. 175, pp. 621-624, 11/30/ 2004.

[44] P. M. Cunio, T. Ishimatsu, J. Keller, Z. Khan, R. Odegard, P. Waswa, *et al.*, "Near-Term Mars Sample Return Using In-Situ Oxygen Generation," in *AIAA SPACE 2007 Conference & Exposition*, 2007, p. 6064.

[45] G. Landis, P. Cunio, T. Ishimatsu, J. Keller, Z. Khan, and R. Odegard, "Mars Sample Return with ISRU," *LPI Contributions,* vol. 1353, p. 3369, 2007.

[46] A. J. Boiron and B. J. Cantwell, "Hybrid Rocket Propulsion and In-Situ Propellant Production for Future Mars Missions," in *49th AIAA/ASME/SAE/ASEE Joint Propulsion Conference*, 2013.

[47] K. J. Yoon, J. W. Son, J. H. Lee, B. K. Kim, H. J. Je, and H. W. Lee, "Performance and Stability of High Temperature Solid Oxide Electrolysis Cells (SOECs) for Hydrogen Production," *ECS Transactions,* vol. 57, pp. 3099-104, / 2013.

[48] S.-E. Yoon, J.-Y. Ahn, B.-K. Kim, and J.-S. Park, "Improvements in co-electrolysis performance and long-term stability of solid oxide electrolysis cells based on ceramic composite cathodes," *International Journal of Hydrogen Energy*, vol. 40, pp. 13558-13565, 10/19/ 2015.

[49] T. L. Cable, J. A. Setlock, S. C. Farmer, and A. J. Eckel, "Regenerative performance of the NASA symmetrical solid oxide fuel cell design," *International Journal of Applied Ceramic Technology*, vol. 8, pp. 1-12, 2011.

[50] T. L. Cable and S. W. Sofie, "A symmetrical, planar SOFC design for NASA's high specific power density requirements," *Journal of Power Sources,* vol. 174, pp. 221-227, 2007.

[51] F. Bidrawn, G. Kim, G. Corre, J. Irvine, J. M. Vohs, and R. J. Gorte, "Efficient reduction of CO2 in a solid oxide electrolyzer," *Electrochemical and Solid-State Letters,* vol. 11, pp. B167-B170, 2008.

[52] S. Li and K. Xie, "Composite oxygen electrode based on LSCF and BSCF for steam electrolysis in a proton-conducting solid oxide electrolyzer," *Journal of The Electrochemical Society*, vol. 160, pp. F224-F233, 2013.

[53] P. Corporation. (2015, 5/1/16). *Solid Oxide Electrolysis*. Available: http://www.paragonsdc.com/life-support/

[54] X. Zhang, J. E. O'Brien, R. C. O'Brien, J. J. Hartvigsen, G. Tao, and G. K. Housley, "Improved durability of SOEC stacks for high temperature electrolysis," *International Journal of Hydrogen Energy,* vol. 38, pp. 20-28, 2013.

[55] A. C. Muscatello, E. Santiago-Maldonado, T. Gibson, R. Devor, and J. Captain, "Evaluation of Mars CO2 Capture and Gas Separation Technologies," 2011.

[56] J. E. O'Brien, "Thermodynamics and Transport Phenomena in High Temperature Steam Electrolysis Cells," *Journal of Heat Transfer,* vol. 134, pp. 031017-031017, 2012.

[57] M. Carmo, D. L. Fritz, J. Mergel, and D. Stolten, "A comprehensive review on PEM water electrolysis," *International Journal of Hydrogen Energy*, vol. 38, pp. 4901-4934, 4/22/ 2013.

[58] K. Zeng and D. Zhang, "Recent progress in alkaline water electrolysis for hydrogen production and applications," *Progress in Energy and Combustion Science,* vol. 36, pp. 307-326, 6// 2010.

[59] O. Yamamoto, "Solid oxide fuel cells: fundamental aspects and prospects," *Electrochimica Acta,* vol. 45, pp. 2423-2435, 5/3/ 2000.

[60] U. F. C. C. s. S. O. F. C. F. Group, "Introduction to Solid Oxide Fuel Cell Button Cell Testing," US Fuel Cell Council, 1100 H Street, NW, Suite 800, Washington, DC 20006 07-015, July 6, 2007 2007.

[61] F. Zhao and A. V. Virkar, "Dependence of polarization in anode-supported solid oxide fuel cells on various cell parameters," *Journal of Power Sources,* vol. 141, pp. 79-95, 2/16/ 2005.

[62] X. Li, *Principles of Fuel Cells*. Great Britain: Taylor & Francis Group, 2006.

[63] F. F. Abdi, L. Han, A. H. M. Smets, M. Zeman, B. Dam, and R. van de Krol, "Efficient solar water splitting by enhanced charge separation in a bismuth vanadate-silicon tandem photoelectrode," *Nat Commun,* vol. 4, 07/29/online 2013.

[64] H. Takenaka, E. Torikai, Y. Kawami, and N. Wakabayashi, "Solid polymer electrolyte water electrolysis," *International Journal of Hydrogen Energy*, vol. 7, pp. 397-403, // 1982.

[65] S. Hu, C. Xiang, S. Haussener, A. D. Berger, and N. S. Lewis, "An analysis of the optimal band gaps of light absorbers in integrated tandem photoelectrochemical water-splitting systems," *Energy & Environmental Science,* vol. 6, pp. 2984-2993, 2013.

[66] A. Hauch, S. D. Ebbesen, S. H. Jensen, and M. Mogensen, "Highly efficient high temperature electrolysis," *Journal of Materials Chemistry,* vol. 18, pp. 2331-2340, 2008.

[67] A. Brisse, J. Schefold, and M. Zahid, "High temperature water electrolysis in solid oxide cells," *International Journal of Hydrogen Energy,* vol. 33, pp. 5375-5382, 10// 2008.

[68] H. Zhang, J. Wang, S. Su, and J. Chen, "Electrochemical performance characteristics and optimum design strategies of a solid oxide electrolysis cell system for carbon dioxide reduction," *International Journal of Hydrogen Energy,* vol. 38, pp. 9609-9618, 2013.

[69] C. M. Stoots, J. E. O'Brien, J. S. Herring, and J. J. Hartvigsen, "Syngas Production via High-Temperature Coelectrolysis of Steam and Carbon Dioxide," *Journal of Fuel Cell Science and Technology,* vol. 6, p. 011014, 2009.

[70] J. Herring, J. Obrien, C. Stoots, G. Hawkes, J. Hartvigsen, and M. Shahnam, "Progress in high-temperature electrolysis for hydrogen production using planar SOFC technology," *International Journal of Hydrogen Energy,* vol. 32, pp. 440-450, 2007.

[71] C. M. Stoots, J. E. O'Brien, K. G. Condie, and J. J. Hartvigsen, "High-temperature electrolysis for large-scale hydrogen production from nuclear energy – Experimental investigations," *International Journal of Hydrogen Energy,* vol. 35, pp. 4861-4870, 5// 2010.

[72] A. Brisse and J. Schefold, "High Temperature Electrolysis at EIFER, Main Achievements at Cell and Stack Level," *Energy Procedia,* vol. 29, pp. 53-63, // 2012.

[73] S. D. Ebbesen, J. Høgh, K. A. Nielsen, J. U. Nielsen, and M. Mogensen, "Durable SOC stacks for production of hydrogen and synthesis gas by high temperature electrolysis," *International Journal of Hydrogen Energy,* vol. 36, pp. 7363-7373, 2011.

[74] J. Mougin, A. Mansuy, A. Chatroux, G. Gousseau, M. Petitjean, M. Reytier, *et al.*, "Enhanced Performance and Durability of a High Temperature Steam Electrolysis Stack," *Fuel Cells,* vol. 13, pp. 623-630, 2013.

[75] J. Mougin, A. Chatroux, K. Couturier, M. Petitjean, M. Reytier, G. Gousseau, *et al.*, "High Temperature Steam Electrolysis Stack with Enhanced Performance and Durability," *Energy Procedia,* vol. 29, pp. 445-454, 2012.

[76] B. Yu, W. Zhang, J. Chen, J. Xu, and S. Wang, "Advance in highly efficient hydrogen production by high temperature steam electrolysis," *Science in China Series B: Chemistry,* vol. 51, pp. 289-304, 2008.

[77] Y. Bo, Z. Wenqiang, X. Jingming, and C. Jing, "Status and research of highly efficient hydrogen production through high temperature steam electrolysis at INET," *International Journal of Hydrogen Energy,* vol. 35, pp. 2829-2835, 2010.

[78] Q. Li, Y. Zheng, W. Guan, L. Jin, C. Xu, and W. G. Wang, "Achieving high-efficiency hydrogen production using planar solid-oxide electrolysis stacks," *International Journal of Hydrogen Energy,* vol. 39, pp. 10833-10842, 2014.

[79] Y. Zheng, Q. Li, W. Guan, C. Xu, W. Wu, and W. G. Wang, "Investigation of 30-cell solid oxide electrolyzer stack modules for hydrogen production," *Ceramics International,* vol. 40, pp. 5801-5809, 2014.

[80] J. Hong, H.-J. Kim, S.-Y. Park, J.-H. Lee, S.-B. Park, J.-H. Lee, *et al.*, "Electrochemical performance and long-term durability of a 200 W-class solid oxide regenerative fuel cell stack," *International Journal of Hydrogen Energy,* vol. 39, pp. 20819-20828, 2014.

[81] S.-D. Kim, J.-H. Yu, D.-W. Seo, I.-S. Han, and S.-K. Woo, "Hydrogen production performance of 3-cell flat-tubular solid oxide electrolysis stack," *International Journal of Hydrogen Energy,* vol. 37, pp. 78-83, 2012.

[82] Y. Shi, Y. Luo, N. Cai, J. Qian, S. Wang, W. Li, *et al.*, "Experimental characterization and modeling of the electrochemical reduction of CO2 in solid oxide electrolysis cells," *Electrochimica Acta,* vol. 88, pp. 644-653, 2013.

[83] J. O. Elliott, R. J. Lipinski, and D. I. Poston, "Design Concept for a Nuclear Reactor-Powered Mars Rover," *AIP Conference Proceedings,* vol. 654, p. 376, 2003.

[84] D. Jiang and P. Zhang, "An Electrical Power System of Mars Rover," in *2014 IEEE Transportation Electrification Conference and Expo, Asia-Pacific (ITEC Asia-Pacific), 31 Aug.-3 Sept. 2014*, Piscataway, NJ, USA, 2014, p. 4 pp.

[85] V. Duboviks, M. Lomberg, R. C. Maher, L. F. Cohen, N. P. Brandon, and G. J. Offer, "Carbon deposition behaviour in metal-infiltrated gadolinia doped ceria electrodes for simulated biogas upgrading in solid oxide electrolysis cells," *Journal of Power Sources,* vol. 293, pp. 912-921, 2015.

[86] Z. Zhan and L. Zhao, "Electrochemical reduction of CO 2 in solid oxide electrolysis cells," *Journal of Power Sources,* vol. 195, pp. 7250-7254, 2010.

[87] Y. Tao, S. D. Ebbesen, and M. Mogensen, "Degradation of solid oxide cells during co-electrolysis of H2O and CO2: Carbon deposition under high current densities," 65 South Main Street, Building D, Pennington, NJ 08534-2839, United States, 2012, pp. 139-151.

[88] R. D. Green, C.-C. Liu, and S. B. Adler, "Carbon dioxide reduction on gadolinia-doped ceria cathodes," *Solid State Ionics,* vol. 179, pp. 647-660, 7// 2008.

[89] S. S. Zumdahl and S. A. Zumdahl, *Chemistry: An Atoms First Approach*: Cengage Learning, 2011.

[90] G. Schiller, R. Henne, M. Lang, and M. Muller, "Development of solid oxide fuel cells (SOFC) for stationary and mobile applications by applying plasma deposition processes,"

in *THERMEC'2003. International Conference on Processing and Manufacturing of Advanced Materials, 7-11 July 2003*, Switzerland, 2003, pp. 2539-44.

[91] P. Moçoteguy and A. Brisse, "A review and comprehensive analysis of degradation mechanisms of solid oxide electrolysis cells," *International journal of hydrogen energy*, vol. 38, pp. 15887-15902, 2013.

[92] S. C. Singhal and K. Kendall, *High-temperature solid oxide fuel cells: fundamentals, design and applications*: Elsevier, 2003.

[93] C. Graves, S. D. Ebbesen, S. H. Jensen, S. B. Simonsen, and M. B. Mogensen, "Eliminating degradation in solid oxide electrochemical cells by reversible operation," *Nature materials*, vol. 14, pp. 239-244, 2015.

[94] M. Ni, "Modeling of a solid oxide electrolysis cell for carbon dioxide electrolysis," *Chemical Engineering Journal*, vol. 164, pp. 246-254, 10/15/ 2010.

[95] J. E. O'Brien, "Large Scale Hydrogen Production from Nuclear Energy using High Temperature Electrolysis," in *2010 14th International Heat Transfer Conference*, 2010, pp. 287-308.

[96] A. O. Isenberg and R. J. Cusick, "Carbon dioxide electrolysis with solid oxide electrolyte cells for oxygen recovery in life support systems," 1988.

[97] C. S. Iacomini and K. Sridhar, "Electrolyzer power requirements for oxidizer production on mars," *Journal of propulsion and power*, vol. 21, pp. 1062-1068, 2005.

[98] J. I. Lunine, J. Chambers, A. Morbidelli, and L. A. Leshin, "The origin of water on Mars," *Icarus*, vol. 165, pp. 1-8, 2003.

[99] C. Chieh. (4/19/2016). *Nernst Equation*. Available: http://www.science.uwaterloo.ca/~cchieh/cact/c123/nernsteq.html

[100] T. Helmenstine. (2014, 3/19/2016). *Nernst Equation Example Problem: Calculate Cell Potential in Nonstandard Conditions*. Available: http://chemistry.about.com/od/workedchemistryproblems/a/Nernst-Equation-Example-Problem.htm

[101] M. R. Leach. (2016, 03/28/2016). *Thermochemistry Synthlet*. Available: http://www.meta-synthesis.com/webbook/51_thermo/Gibbs_synthlet_build.php

Appendix A

Matlab Code

```
%Carbon Dioxide Nernst Potential Calculation

%By Timothy Bernadowski

%Based on code by Can Zhou

clear all;

clear clc;

R = 8.3144621;                          %parameters

n = 2;                                  %2 electrons

F = 96487;                              %Faraday's constant

%%

%Temperature Ranges

t1 = [298 400:100:1800];                %temperatures from 600-1800K



%Gibb's Free Energy

G1 = [257.2 248.4 239.7 231.1 222.4 213.8 205.1 196.5 187.8...

    179.2 170.5 161.9 153.2 144.6 135.9 127.3];
```

```
G2 = [137.2 146.3 155.2 164.1 173.1 182   191   199.9 208.8...
     217.8 226.7 235.6 244.6 253.5 262.4 271.4];
G3 = [394.4 394.7 394.9 395.2 395.5 395.8 396.1 396.4 396.7...
     396.9 397.2 397.5 397.8 398.1 398.4 398.7];
%Electrolysis Potential Equations (at standard pressure)
E1 = -1000*G1/(n*F);                          %CO2 -> CO + 0.5 O2
E2 = -1000*G2/(n*F);                          %CO  -> C  + 0.5 O2
E3 = -1000*G3/(2*n*F);                         %CO2 -> C  + O2
%Nernst Potential for Standard Conditions Graphs
figure(1)
 plot(t1-273, -E1, 'b','Linewidth',3);
 hold on
 plot(t1-273, -E2, 'c','Linewidth',3);
 hold on
 plot(t1-273, -E3, 'k','Linewidth',3);
 hold on
 xlabel('Temperature (^oC)');
```

```
 grid on
 axis([0 1600 0.6 1.7]);
 ylabel('Electrolysis Potential (V)');
 legend('CO_2 -> CO + 0.5 O_2', 'CO -> C + 0.5 O_2', 'CO_2 -> C + O_2');
%%
%Modifying for the Pressure & Various Concentrations
%For the CO2 -> CO + 0.5 O2 equation
K=(0.9)^1*(0.1)^-1*0.21^-0.5*((0.005683)^-0.5);
 Ep1=E1-R*t1/n/F*log(K);
K=(0.7)^1*(0.3)^-1*0.21^-0.5*((0.005683)^-0.5);
 Ep2=E1-R*t1/n/F*log(K);
K=(0.5)^1*(0.5)^-1*0.21^-0.5*((0.005683)^-0.5);
 Ep3=E1-R*t1/n/F*log(K);
K=(0.3)^1*(0.7)^-1*0.21^-0.5*((0.005683)^-0.5);
 Ep4=E1-R*t1/n/F*log(K);
%Modifying the Other Reactions
K=(0.1)^1*(1)^-1*0.21^-0.5*((0.005683)^-0.5);          %CO  -> C + 0.5 O2
```

```
Ep5=E2-R*t1/n/F*log(K);

K=(0.9)^1*(1)^-1*0.21^-1*((0.005683)^-1);              %CO2 -> C + O2

Ep6=E3-R*t1/(2*n)/F*log(K);

 %Creating the necessary graphs

figure(2)

 plot(t1-273,-Ep1,'g','LineWidth',3);                  %line style

 hold on

 plot(t1-273,-Ep5,'c','Linewidth',3);

 hold on

 plot(t1-273,-Ep6,'k','Linewidth',3);

 grid on

 axis([0 1600 0.6 1.7]);

 xlabel('Temperature (^oC)');

 ylabel('Electrolysis potential (V)');

 title('Nernst Potential with Different CO_2 Content: 90% CO_2 & 10% CO');

 legend('90% CO_2 & 10% CO','CO -> C + 0.5 O_2','CO_2 -> C + O_2');

 %For 70% CO2 - 30% CO
```

```
K=(0.3)^1*(1)^-1*0.21^-0.5*((0.005683)^-0.5);          %CO  -> C + 0.5 O2

Ep5=E2-R*t1/n/F*log(K);

K=(0.7)^1*(1)^-1*0.21^-1*((0.005683)^-1);              %CO2 -> C + O2

Ep6=E3-R*t1/(2*n)/F*log(K);

figure(3)

 plot(t1-273,-Ep2,'r','LineWidth',3);                  %line style

 hold on

 plot(t1-273,-Ep5,'c','Linewidth',3);

 hold on

 plot(t1-273,-Ep6,'k','Linewidth',3);

 grid on

 axis([0 1600 0.6 1.7]);

 xlabel('Temperature (^oC)');

 ylabel('Electrolysis potential (V)');

 title('Nernst Potential with Different CO_2 Content: 70% CO_2 & 30% CO');

 legend('70% CO_2 & 30% CO','CO -> C + 0.5 O_2','CO_2 -> C + O_2');

%For 50% CO2 - 50% CO
```

```
K=(0.5)^1*(1)^-1*0.21^-0.5*((0.005683)^-0.5);          %CO  -> C + 0.5 O2

Ep5=E2-R*t1/n/F*log(K);

K=(0.5)^1*(1)^-1*0.21^-1*((0.005683)^-1);              %CO2 -> C + O2

Ep6=E3-R*t1/(2*n)/F*log(K);

figure(4)

 plot(t1-273,-Ep3,'b','LineWidth',3);                  %line style

 hold on

 plot(t1-273,-Ep5,'c','Linewidth',3);

 hold on

 plot(t1-273,-Ep6,'k','Linewidth',3);

 grid on

 axis([0 1600 0.6 1.7]);

 xlabel('Temperature (^oC)');

 ylabel('Electrolysis potential (V)');

 title('Nernst Potential with Different CO_2 Content: 50% CO_2 & 50% CO');

 legend('50% CO_2 & 50% CO','CO -> C + 0.5 O_2','CO_2 -> C + O_2');

%For 30% CO2 - 70% CO
```

```
K=(0.7)^1*(1)^-1*0.21^-0.5*((0.005683)^-0.5);          %CO  -> C + 0.5 O2

Ep5=E2-R*t1/n/F*log(K);

K=(0.3)^1*(1)^-1*0.21^-1*((0.005683)^-1);              %CO2 -> C + O2

Ep6=E3-R*t1/(2*n)/F*log(K);

figure(5)

 plot(t1-273,-Ep4,'y','LineWidth',3);                  %line style

 hold on

 plot(t1-273,-Ep5,'c','Linewidth',3);

 hold on

 plot(t1-273,-Ep6,'k','Linewidth',3);

 grid on

 axis([0 1600 0.6 1.7]);

 xlabel('Temperature (^oC)');

 ylabel('Electrolysis potential (V)');

 title('Nernst Potential with Different CO_2 Content: 30% CO_2 & 70% CO');

 legend('30% CO_2 & 70% CO','CO -> C + 0.5 O_2','CO_2 -> C + O_2');
```

Appendix B

Oxygen Pump Mode Data

Voltage (Volts)	Current (Amps)	Power (Watts)
0.01	0.0014	0.000014
0.02	0.0064	0.000128
0.03	0.0121	0.000363
0.04	0.0175	0.0007
0.05	0.0226	0.00113
0.06	0.0274	0.001644
0.07	0.0323	0.002261
0.08	0.0369	0.002952
0.09	0.0414	0.003726
0.1	0.0455	0.00455
0.2	0.0752	0.01504
0.3	0.0883	0.02649
0.4	0.0958	0.03832
0.5	0.1002	0.0501
0.6	0.1089	0.06534
0.7	0.1154	0.08078
0.8	0.1232	0.09856
0.9	0.1334	0.12006

Vita

TIMOTHY A. BERNADOWSKI, JR.

1015 W 50th Street
Apt. 3
Norfolk, VA 23508

Mobile Tel: (804) 347-9520
School Email: tbern008@odu.edu
Personal Email: tjbernad@comcast.net

EDUCATION

Master of Science (Candidate), Mechanical Engineering, Old Dominion University, Norfolk, VA. Technical Area: Thermodynamics and Energy. Current GPA: 3.74/4.0. Master's Thesis: *Carbon Deposition During Oxygen Production Using High Temperature Electrolysis and Mitigation Methods*, April, 2016. Advisor: Dr. Xiaoyu Zhang.

Bachelor of Science, Mechanical Engineering, Old Dominion University, Norfolk, VA. Technical Area: Power and Energy. Final GPA: 3.81/4.0. Senior Project: *To convert a UAV from battery power to fuel cell power in order to maximize flight time and energy efficiency*, May, 2015.

HONORS AND AWARDS

Virginia Space Grant Consortium Graduate STEM Research Fellowship, $6,000/year, 2015-2016.
Old Dominion University (ODU) Dean's Scholarship, 2011-2015.
ODU Alumni Association Adam Thoroughgood Scholarship, 2011-2015.
American Society of Heating, Refrigeration & Air-Conditioning Engineers (Richmond, VA) Scholarship, 2011.
St. Paul's Catholic Church Scholarship, 2011.
Eagle Scout, 2010.

RELATED WORK EXPERIENCE

2015-2016: **Graduate Teaching Assistant**, Department of Mechanical & Aerospace Engineering, Old Dominion University. Responsible for assisting professors in grading, cataloging, tutoring students, communication, proctoring examinations, and in some cases providing instruction to students.

Summer 2015: **Mechanical Design Analysis Intern**, Nuclear Design Engineering Services, Dominion Resources. Performed calculations & analysis related to North Anna Power Station's Air Operated Valves & ASME Appendix IV Implementation. Assisted with system level calculations and data analysis.

Summer 2014: **Probabilistic Risk Assessment (PRA) Engineering Intern**, Nuclear Safety Analysis & Fuel, Dominion Resources. Assisted with the Internal Flooding element of Surry Nuclear Power Station PRA Model Update, including creation

of drawings showing station's flood areas, data collection of flood sources and scenarios, data evaluation in spreadsheets and documents, and outlining an internal flooding database creation project.